

**POLITECNICO DI TORINO**

**Corso di Laurea Magistrale  
in Ingegneria Biomedica**

**Tesi di Laurea Magistrale**

**Shear-thinning biomaterial for  
chemoembolization:  
design, characterization and drug release  
evaluation**



**Relatore**

Prof. Danilo Demarchi

**Candidato**

Marika Sperduti

A.A. 2017/18



*The work presented in this thesis has been carried out at the Khademhosseini Laboratory of Boston, in collaboration with Harvard University, Massachusetts Institute of Technology, Harvard-MIT Health Sciences and Technology and Brigham and Women's Hospital.*



## Contents

<b>Abstract.....</b>	<b>I</b>
<b>1 Introduction .....</b>	<b>1</b>
<b>2 Material design.....</b>	<b>8</b>
2.1 Materials .....	8
2.1.1 Functionalization .....	12
2.2 Shear-thinning biomaterial preparation.....	14
2.3 Material reproducibility.....	18
2.4 Material optimization .....	21
<b>3 In vitro characterization.....</b>	<b>30</b>
3.1 Injectability.....	30
3.2 Degradation.....	32
3.3 Swelling.....	35
3.4 Shelf life .....	38
3.5 Occlusion pressure .....	43
<b>4 Drug release .....</b>	<b>46</b>
4.1 Experiment setup.....	46
4.2 Results .....	53
4.3 Experiment optimization .....	57
<b>5 Conclusions .....</b>	<b>61</b>
5.1 Future directions .....	63
<b>List of Figures .....</b>	<b>64</b>
<b>Bibliography .....</b>	<b>69</b>

## **Abstract**

The hepatocellular carcinoma (HCC) is one of the most lethal and prevalent cancer in the worldwide. Its high vascularization, together with the unique dual blood supply of the liver, have led to an increasing use of the transarterial chemoembolization (TACE) for the treatment of unresectable HCC. The TACE is a promising clinical procedure, that allow the occlusion of the tumor vasculature through the injection of a mixture of embolic agents and chemotherapeutic drugs. The application of this technique leads to the consequent tumor necrosis and to the simultaneous selective drug delivery, decreasing its side effects and rising its chemotherapeutic efficiency. Nowadays, there are multiple available materials to induce the vascular embolization, even if most of them are not able to present a concomitant strong occlusion and easy injectability in the microvasculature. Herein, it is presented a new shear-thinning biomaterial, composed of laponite and gelatin, for the chemoembolization of the hepatocellular carcinoma. The distinctive shear-thinning behavior of the material, enable it to be easily injectable and at the same time to strongly occlude the microvasculature. More specifically, there were analyzed three different compositions of the material, respectively labeled as 6NC75, 5NC75 and 4NC75. In this labelling the first number represents the percentage (w/w) of solid particles, while the second number stands for the percentage (w/w) of the solid particles made up of laponite. These three materials have been characterized with multiple in vitro experiments, showing promising results. Firstly, there were demonstrated their homogeneity and reproducibility, by analyzing the force necessary to inject the materials through a 5 F catheter having a length of 65 cm. It was also proved their ability to be easily injectable in micro tubes, having an inner diameter between 50  $\mu\text{m}$  and 300  $\mu\text{m}$ , in order to simulate the microvasculature of the tumor. Furthermore, it was shown how they can avoid the phenomena of swelling and degradation once that they are incubated at 37 °C together with a phosphate buffer saline solution (PBS). Moreover, there were carried out some studies on the shelf life of the materials, showing that the best way to preserve their properties is to store them in a refrigerated place. It was also analyzed their ability to withstand under pressure higher than the systolic pressure

in different sizes micro tubes, having an inner diameter comparable to the tumor microvasculature. The results showed a different degree of occlusion depending on their composition, suggesting a potential application to occlude the vascularization at different levels, based on their composition. Finally, it is reported a study on the functionalization of the 6NC75 with the doxorubicin, one of the most common chemotherapeutic drugs. Its release profile was analyzed, showing a greater release when the material was incubated in a medium with a pH able to simulate the tumor environment (pH 5.2), rather than when it was incubated with a medium that simulate the physiological environment (pH 7.4). Therefore, this hydrogel could provide a promising alternative gel-based embolic agent with a great potential for the chemoembolization.

## Abstract

Il carcinoma epatocellulare (HCC) è uno dei tumori più letali e diffusi in tutto il mondo. La sua elevata vascolarizzazione, insieme alla peculiare doppia alimentazione del fegato, hanno portato ad un utilizzo sempre maggiore della chemoembolizzazione trans-arteriale (TACE) come tecnica per il trattamento di HCC non resecabili. La TACE è una promettente procedura clinica, che consente l'occlusione dei vasi sanguigni di un tumore tramite la somministrazione di una miscela di agenti embolici con farmaci chemioterapici. L'applicazione di tale tecnica porta alla conseguente necrosi del tumore e alla simultanea somministrazione selettiva del farmaco, diminuendone gli effetti collaterali e aumentandone l'efficacia chemioterapica. Ad oggi, esistono numerosi materiali disponibili sul mercato per poter essere impiegati nell'embolizzazione vascolare, molti dei quali però non sono in grado di fornire una contemporanea buona occlusione e facile abilità di essere iniettati nel microcircolo. In questo elaborato viene presentato un nuovo biomateriale pseudoplastico, composto da laponite e gelatina, per la chemoembolizzazione del carcinoma epatocellulare. Il caratteristico comportamento pseudoplastico di tale materiale, gli consente di essere facilmente iniettabile e allo stesso tempo di occludere efficacemente la micro vascolarizzazione. In particolare, sono state analizzate tre differenti composizioni del materiale, chiamati rispettivamente 6NC75, 5NC75 e 4NC75. In tale denominazione il primo numero sta a rappresentare la percentuale (p/p) di contenuto solido, mentre il secondo numero rappresenta la percentuale (p/p) di contenuto solido costituito da laponite. Tali materiali sono stati caratterizzati con molteplici esperimenti in vitro, ottenendo dei promettenti risultati. Innanzi tutto, è stata confermata la loro omogeneità e riproducibilità, valutando la forza necessaria per iniettarli in un catetere 5 F di 65 cm di lunghezza. È stata inoltre provata la loro capacità di essere facilmente iniettabili in micro tubi, aventi un diametro interno compreso tra i 50  $\mu\text{m}$  e 300  $\mu\text{m}$ , confrontabile con quello della microcircolazione tumorale. Oltre a ciò, è stata dimostrata l'assenza di fenomeni di swelling e degradazione in campioni di materiale incubati a 37 °C in contatto con una soluzione tampone fosfato salino (PBS). Sono stati poi effettuati diversi studi per

analizzare le possibili modalità di conservazione dei materiali, dai quali si è evinto che il modo migliore per poter preservare le loro proprietà è il loro stoccaggio a basse temperature. Successivamente è stata studiata la loro abilità di resistere a pressioni maggiori di quella sistolica, una volta posizionati in micro tubi aventi dimensioni paragonabili a quelle della microcircolazione tumorale. I risultati hanno dimostrato una differente capacità di occlusione a seconda della composizione, suggerendo una loro potenziale applicazione a differenti livelli della vascolarizzazione, a seconda della composizione. Infine, è stato riportato uno studio sulla funzionalizzazione del 6NC75 con la doxorubicina, uno dei più comunemente impiegati farmaci chemioterapici. Dai risultati si può notare un rilascio maggiore del farmaco per il materiale incubato con un mezzo avente un pH tale da simulare l'ambiente tumorale (pH 5.2), rispetto al materiale in contatto con un mezzo in grado di simulare l'ambiente fisiologico (pH 7.4). Pertanto, questo idrogel potrebbe rappresentare una promettente alternativa come agente embolico a base di gel, con un buon potenziale per la chemoembolizzazione.

# 1 Introduction

In the last century, the cancer has had an exponential increase as one of the leading causes of death worldwide. This has led to develop new techniques with the purpose of fighting the most aggressive disease of our years.

The aim of this project is to develop a new shear-thinning biomaterial for chemoembolization of the cancer, in particular as regards the hepatic tumor. The shear-thinning behavior is a unique property of the non-Newtonian fluids, that allow them to decrease their viscosity when undergo to a shear-strain and rapidly recover their mechanical properties when the shear-strain is removed (shear-healing). Whereas, with the term biomaterial is indicated a substance that can be introduced in the body tissues as a part of a medical device or in order to replace any tissue, organ or function of the body.

The hepatic cancer embodies different diseases of the liver, which include epithelioid hemangioendothelioma, hepatoblastoma, bile duct cystadenocarcinoma, intrahepatic bile duct carcinoma (cholangiocarcinoma), hemangiosarcoma and hepatocellular carcinoma (HCC). Between these, the HCC represents the 83% of all the cases. The hepatocellular carcinoma, a progressive tumor, is the sixth most widespread cancer in the world and the third most common cause of cancer-related deaths. Its incident varies around the world, the majority of HCC occur in Sub-Saharan Africa, southeast Asia and East Asia, whereas in North America, USA, south America, Europa, Australia and New Zealand there is a lower incidence of HCC. The global different distribution of the HCC is closely dependent on the variation of the risk factors. The 80% of HCC are caused by chronic hepatitis B (HBV) or C (HCV) viral infections, thus, the countries that present a higher presence of HBV or HCV, are those with a higher percentage of HCC [1] [2] [3] [4].

The cancer generates a series of genetic and epigenetic diseases characterized by the uncontrolled proliferation of cells. An important role in the tumor growth is played by the angiogenesis and lymphangiogenesis, that allow the nutrition of the cancer and the expulsion of waste products [5]. The cancerous cells grow faster than the vasculature that gives them the nutrition, therefore, during its

grow, the solid tumor begins to be subject to hypoxia. In this condition, the hypoxia inducible factor (HIF-1) produce a variety of glycolytic enzymes and glucose transporters, such as GLUT1 and GLUT2, that lead the tumor to stay alive until the vascularization is completed. Furthermore, an important effect of the HIF-1, is its ability to induce the transcription of the vascular endothelial growth factor (VEGF), which is able to promote the angiogenesis in a hypoxic area (*figure 1*). The formation of new blood vessels generates an abnormal angioarchitecture, more dense and chaotic than a healthy one, distinctive of the presence of a cancer diseases as the HCC (*figure 2*).

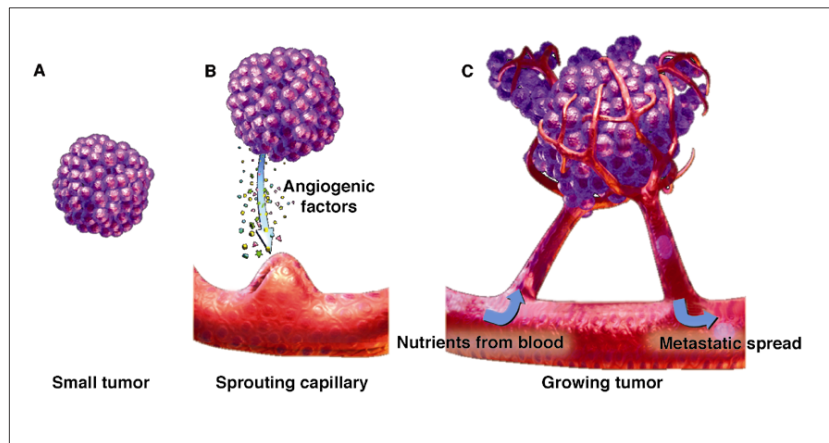


**Figure 1** - Angiogenesis of the tumor. A) Tumor at the first stadium, without vascularization; B) Hypoxia induce the production of angiogenic factors that stimulate the angiogenesis; C) Vascularized tumor. (Source: <http://www.mdpi.com/1422-0067/18/9/1967/htm>)

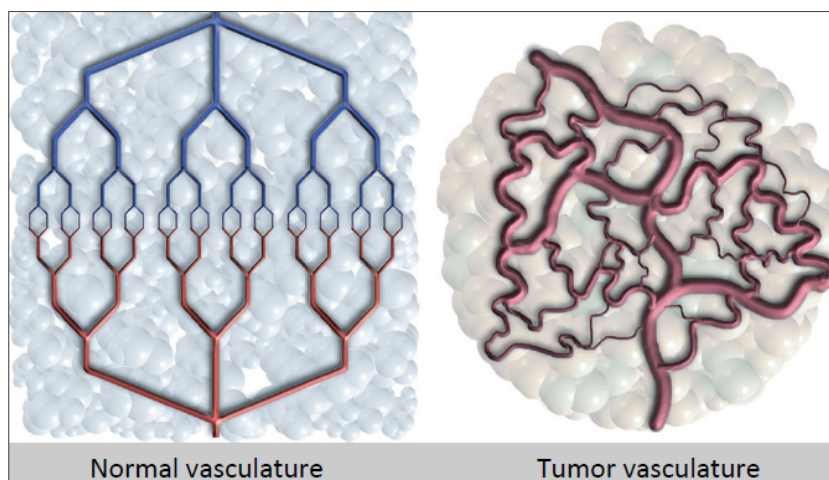


**Figure 2** - Comparison between a normal organized vascularization and the abnormal vascularization of the tumor. (Source: <http://memorize.com/ebme-unit-1-cancer-case-study/ndifranco94>).

In the hepatic angiogenesis the vast majority of the new vessels originate from the portal vein and prone to establish a connection between it and the hepatic veins [6] [7]. A unique characteristic of the liver is its dual blood supply. The liver is the largest organ of the body and receives around the 25% of the total body's blood supply from two different inflow: the portal vein and the hepatic artery. Its circulation includes also an efferent system, represented by the hepatic veins. The portal vein delivers about the 70% of the parenchyma blood supply, that is a partly deoxygenated but nutrient-rich blood. The portal vein is a valve-less vessel that drain the blood from the capillary system of most of the other organs. The remaining 30% of the oxygenated blood supply is delivered to the liver from the hepatic artery. Even if the blood from the portal vein is mostly deoxygenated, it provides more than the 50% of the hepatic oxygen requirement, due to its high flow rate. Moreover, there is a direct communication between the two vascular systems that allows the hepatic artery to adjust its blood flow in response to changes in the flow of the portal vein. The dual blood supply of the liver represents a unique feature of its vascularization that allow a distinctly regulation of the blood flow [8] [9].

The prognosis of hepatocellular carcinoma strictly depends on the tumor stage at the time of the diagnosis and on the possible treatment that can be provided. In the last two decades, an array of new treatments for the HCC have been developed, instead of the classical surgical resection or transplantation, which are still largely used but applicable to a limited set of patients.

The current treatment options for HCC are the following [1] [3] [10]:

- *Resection*, is a potentially curative treatment but it is only applicable to 5-10% of the patients due to the restrictive selection criteria required. Moreover, 70% of the cases after 5 years present a high risk of developing cancer recurrence from the residual liver tissue;
- *Transplantation*, consists in the removal of the whole liver, establishing a definitive treatment. However, the candidates must be considered eligible<sup>1</sup>

---

<sup>1</sup> The candidates are considered eligible if they fulfill the Milan criteria ("a single tumor with less than 5 cm in diameter, or up to three lesions with the largest one having no more than 3 cm in diameter").



for the transplantation using restrictive criteria. Furthermore, a transplant delay, with a worsening in the liver conditions that can lead the patient to be no more eligible, is imposed by the limited number of donors. To overcome this problem, living donors have been introduced increasing the number of possible liver donations. Although, with living donors there is a considerable risk of mortality and morbidity of the donor himself and an increasing recurrence in the patient (due to the transplant even in patient who were not eligible for deceased donor liver transplantation);

- *Radiofrequency ablation*, is a technique that lead to the necrosis of the tumor by temperature modification, using the radiofrequency. It is possible to induce the ablation using other sources, like microwave or laser, or by the injection of chemical agents such as ethanol. Among all these ablations, the radiofrequency is the most common used since it is also the most effective, reaching 98% of total tumor necrosis. However, it can be used only for the treatment of small tumors (< 3 cm in size) that are not eligible for transplantation. The overall survivals are around 70%, showing a similar efficacy to the resection technique, but with a lower complication rate;
- *Pharmacological and chemotherapeutic agent*, the use of these agents is limited since most of the HCCs are resistant to the classic chemotherapeutic drugs and present a low tolerance due to the liver dysfunction;
- *Transarterial radioembolization*, consists in a selective administration, through an intra-arterial injection, of microspheres loaded with radioactive compound. The therapeutic effect does not depend on the embolization of the vessels but on the radiation carried by the microspheres. This technique has been recently introduced in the clinical practices so there are not enough results to show its efficiency. However, it is incising being use for the treatment of unresectable and multifocal HCC;
- *Transarterial Chemoembolization (TACE)*, is a clinical procedure to occlude the vasculature of the tumor by injecting a mixture of occluding agent and chemotherapeutic drug inside of the target tumor. It is used for the HCC that are unresectable or that cannot be treated with the ablative

technique. It is also indicated as a treatment before the liver transplantation to reduce or maintain the tumor size.

It is possible to use the TACE in the HCC thanks to the dual blood supply of the liver. The normal parenchyma of the liver derives two-thirds of its blood supply from the portal vein and the remainder from the hepatic artery. Whereas, the malignant lesions, derives 90% of their blood supply from the hepatic artery. Thus, the normal hepatic parenchyma is preserved even if all the blood supply is diverted away from the tumor and a high concentrated chemotherapeutic drug is delivered to the tumor tissues [8] [11]. This technique, despite the high concentration of the chemotherapeutic drug, consents to reduce the side effects and cytotoxicity associate with the drug since it is locally injected into the tumor tissue. Moreover, the drug is not wash out since the artery is blocked and the embolic agent leads to the ischemia and consequently necrosis of the tumor.

The procedure for the injection of the chemo-embolic agent is performed in angiography to confirm the anatomy and check the correct position of the catheter before that the material is injected. The material is delivered to the tumor vasculature with the use of a catheter, which should have a diameter that is at least half of the vessel one. The catheter is inserted into the femoral artery and superselectively advance until it reaches the hepatic artery that feeds the tumor. When the catheter is correctly positioned for the treatment, the material is injected and the tumor feeding vasculature is blocked (*figure 3*) [8].

There are multiple available materials to induce the vessels occlusion. They can be differentiated from two main parameters: the dimensions of the vessels that have to be occluded and whether they need to produce a permanent or temporary occlusion. The size of the embolic agent is an important factor since, when the larger vessels are occluded, a hypoxia is generated that promotes the angiogenesis resulting in a revascularization of the tumor. Whereas, the occlusion of the end-branches of the hepatic artery can prevent the development of a collateral arterial flow to the tumor. The *gelatin sponge* was the first embolic agent to be used in the late 1970s and it is still widely used for temporary occlusion. It is composed of purified porcine-derived gelatin that can be sold as a powder or as sheets that should be cut before use. The particles size is around the millimeter, allowing them

to occlude the larger artery. When the gelatin sponge is in the form of powder, it is able to reach the smaller vessels. However, it can also penetrate more deeply into the tissues resulting in untargeted embolization. Another embolic agent that is currently used for the TACE is the non-spherical polyvinyl alcohol *PVA*, employed for permanent or semi-permanent occlusion with different particles shapes and sizes, from 10  $\mu\text{m}$  to 1500  $\mu\text{m}$ . However, due to the different sizes and shapes, these particles tend to aggregate together by blocking the catheter and making it difficult to go down in the vessel size. To overcome these issues, the microspheres with calibrated size have been developed. They can be realized with a range of different sizes and, depending on the size, can penetrate deeper in the vessels. The *fluid embolic agents*, as biological glues and gelling solutions, are also used for the TACE. They are able to reach and occlude the microvasculature, adapting their shape to the vessels before becoming more solid. The biological glues are composed of one or more liquid components that solidified as soon as they polymerized. The polymerization, since is generally anionic, occurs when the glues come in contact with the body fluid. Whereas, the gelling solutions are composed of a polymer, that solidified in situ, and a solvent that is replaced by the water when it reaches the target vessel. The fluid embolic agents are able to occlude very small vessels ( $<100 \mu\text{m}$ ), allowing to overcome the revascularization of the tumor that represent an important problem for the chancer embolization [12] [8].

In this project it has been developed a new injectable, shear-thinning hydrogel for the chemoembolization of the liver tumor HCC. It has been realized with the aim of eradicating the tumor, since the absence of a vascular support can lead the tumor to necrosis and the synergistic release of a chemotherapeutic drug in loco can have a more efficient effect on it. The developed material was designed in order to be easily injectable in the microvasculature of the tumor with an inner diameter of less than 300  $\mu\text{m}$ . At the same time, it should be able to occlude the target vessels and simultaneously release a chemotherapeutic drug.

First of all, the individual components of the material and their interactions are analyzed. Whereupon, there are described the procedures to realize three different compositions of the material and a way to optimize these procedures. The three different materials produced are therefore characterized with some in vitro

experiments. It was tested the possibility of their degradation or absorption of body fluid by simulating the body environment. Moreover, was analyzed the feasibility to preserve the properties of the materials for a long period of time and also their ability to occlude different sizes micro vessels. Finally, it is reported the study of the drug release from the material, investigating different ways of functionalization. Furthermore, was analyzed the drug release from two different environments, the body and the tumor, which were simulated using two different pH solutions.

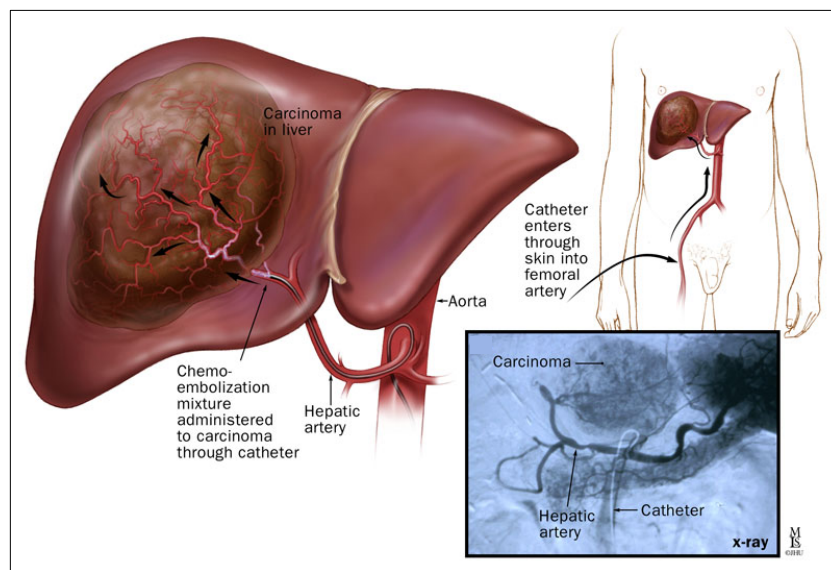


**Figure 3** - Chemoembolization of the liver carcinoma procedure.

(Source: [https://www.hopkinsmedicine.org/liver\\_tumor\\_center/treatments/intraarterial\\_therapies/index.html](https://www.hopkinsmedicine.org/liver_tumor_center/treatments/intraarterial_therapies/index.html))

## 2 Material design

In this chapter there are described the single components of the shear-thinning biomaterial (STB). It is also defined the procedure to produce three different compositions of the STB. Furthermore, there are shown the reproducibility of the realized materials and a trial to optimize the protocol used to produce them.

### 2.1 Materials

Hydrogels are three-dimensional polymeric networks, able to hold a grate quantity of water while maintaining their structural integrity. Herein, we are introducing a shear-thinning hydrogel that is easily injectable under modest pressure and that is able, after the release of the applied shear stress, to rebuild its structure and become more solid and static. It is realized with laponite, a synthetic silicate, and gelatin, a polypeptide obtained by the hydrolytic collagen degradation.

Laponite<sup>2</sup> (hydrous sodium lithium magnesium silicate) is a synthetic crystalline layered silicate colloid, made up of two-dimensional disc-shaped nanoparticles. It has a structure that is very similar to the natural mineral clay hectorite. Its most important property is its shear-thinning behavior, that acquires when is disperse in water. It is also highly biocompatible, easily able to form a gel and it degrades into non-toxic products, such as Na<sup>+</sup>, Mg<sup>2+</sup>, Si(OH)<sub>4</sub> and Li<sup>+</sup>. The single laponite crystal has a typically diameter of ~ 25 nm and a thickness of ~ 0.92 nm. Within each crystal there is a sheet of octahedrally coordinated magnesium oxide, sandwiched between two parallel layers of tetrahedrally coordinated silica. The empirical formula (Na<sup>+</sup><sub>0.7</sub>[Si<sub>8</sub>Mg<sub>5.5</sub>Li<sub>0.3</sub>)O<sub>20</sub>(OH)<sub>4</sub>]<sup>-0.7</sup>) shows the presence of lithium cations (Li<sup>+</sup>), that randomly substitute the magnesium one (Mg<sup>2+</sup>), giving a net negative charge to the faces of the disks. This negative charge is balanced by the interlayer cations of sodium. Whereas the edges of the disks are positively charged.

---

<sup>2</sup> Laponite XLG-XR, purchased from BYK Additives Inc, Gonzales TX.

In the dry powder, the crystals of laponite, are arranged in stacks that are electrostatically hold together by sharing interlayer sodium ions.

When laponite is dispersed in water, the sodium ions ( $\text{Na}^+$ ) dissociate, forming a clear colloidal dispersion with a permanent negative charge on the particles surfaces [12] [13]. In these conditions, the osmotic pressure from the bulk of water pulls the single crystal away and the stacked structure exfoliate in single particles. The single particles can interact each other with a face to edge attraction. This process is responsible of the gelation of the laponite suspension, generating a “house of card” structure which is highly thixotropic<sup>3</sup> (*figure 4*) [15, 16]. When the laponite is completely exfoliated it results in a transparent gel. The formation of a stable gel depends on the solid concentration and incubation time. It is known that laponite with a concentration higher than 3% (w/v), forms a gel after 15 minutes of vigorous mixing at room temperature. It is possible to obtain the gelation also with a lower concentration by increasing the mixing time. It has been previously investigated that 0.3% (w/v) of laponite forms a gel after 6 months of incubation [17].

The charge on the edges of the laponite dispersed in water, which contains predominantly  $\text{MgOH}$ , is highly pH dependent. The point of zero charge of the edges of the laponite has been demonstrated to be at pH 11, so depending on the pH of the medium, either  $\text{OH}^-$  or  $\text{H}^+$  ions are dissociated. Dissociation of  $\text{OH}^-$  from the edges occurred below the isoelectric pH, causing an increase in pH of the dispersion. Therefore, the presence of ions in the solvent strongly influences the final pH and the stability of the hydrogel during its formation. Moreover, it has been noticed in previous studies that the leaching of magnesium ions increases with decreases in pH. The presence of ions in the solution results in shielding the surface charge of the nanoplates and hindering the self-assembly of them into a “house of cards” structure [17]. In order to obtain a shear-thinning biomaterial (STB), when the laponite is fully exfoliated it is mixed with an aqueous solution of gelatin from porcine skin (type A).

---

<sup>3</sup> Thixotropic is a time dependent shear-thinning property of some non-Newtonian fluid, which decres their viscosity under the application of shear stress and take a fixed time to return to a more viscous state.

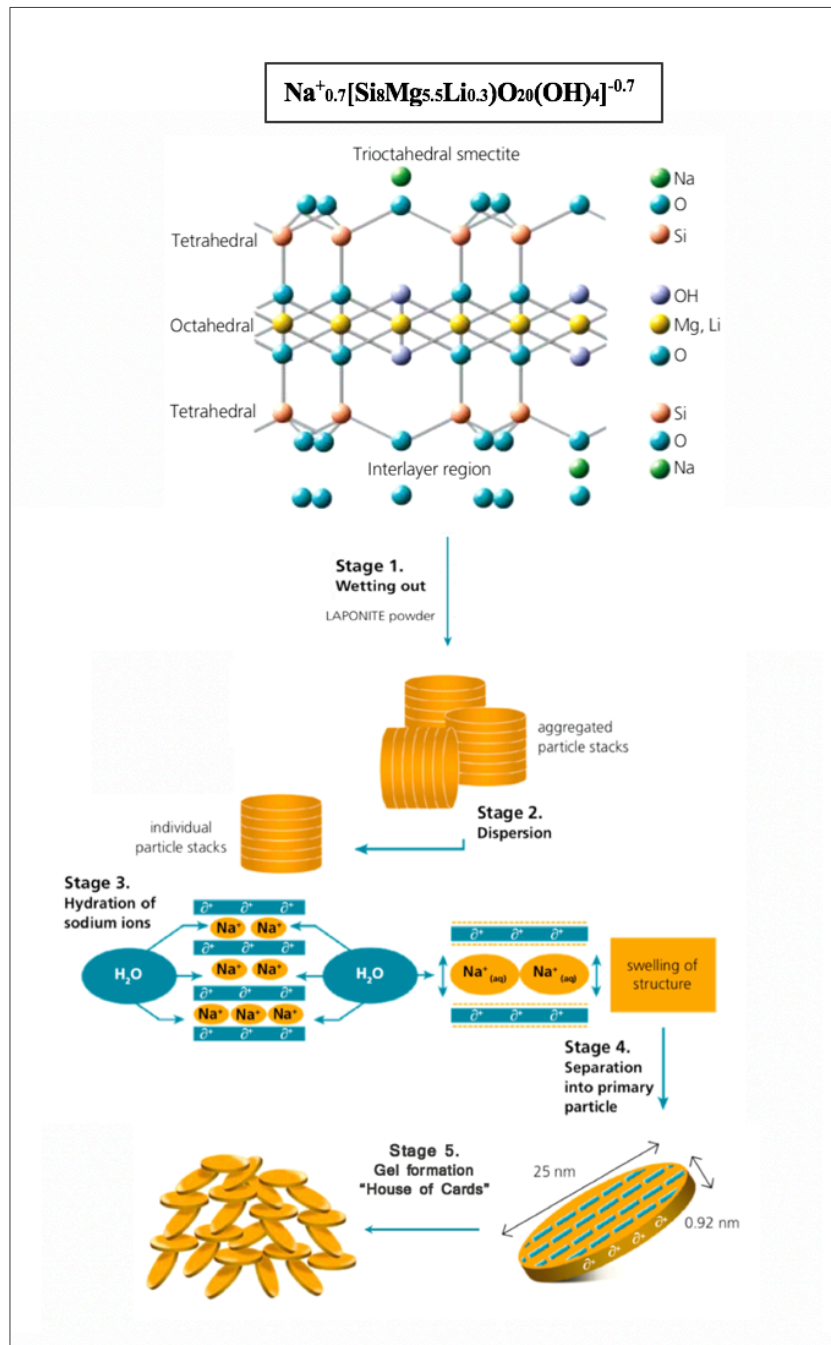


**Figure 4** - Schematic representation of the gelation of the laponite. It shows the chemical structure of a single disk of laponite and the single steps from the dry state to the "house of cards" structure of the laponite when is dispersed in water. (Source: BYK, technical information B-RI 21, LAPONITE-Performance Additives)

The gelatin<sup>4</sup> (type A, from porcine skin) is a denatured collagen, positively charged, with an excellent biocompatibility, biodegradation and hydrophilicity. In structure and chemical composition, it mimics the native extracellular matrix (ECM). It is a heterogeneous mixture of water soluble proteins of the collagen with a high weight molecular mass. The proteins are extracted by boiling in water: skin, bones ligaments etc.. This procedure is delivered from an acid-cured tissue [19, 20]. The vigorous mixing of the laponite and gelatin in water, generates a physically crosslinking hydrogel, with a strong interaction between the positive charges of the gelatin chains and the negative charges on the two sides of the nanoplates of the laponite (*figure 5*). Indeed, previous study have shown a negative zeta potential, around - 40 mV for the laponite, and a positive one of 10 mV for the gelatin. Moreover, after the formation of the final STB, the zeta potential is demonstrated to be steel negative [20].

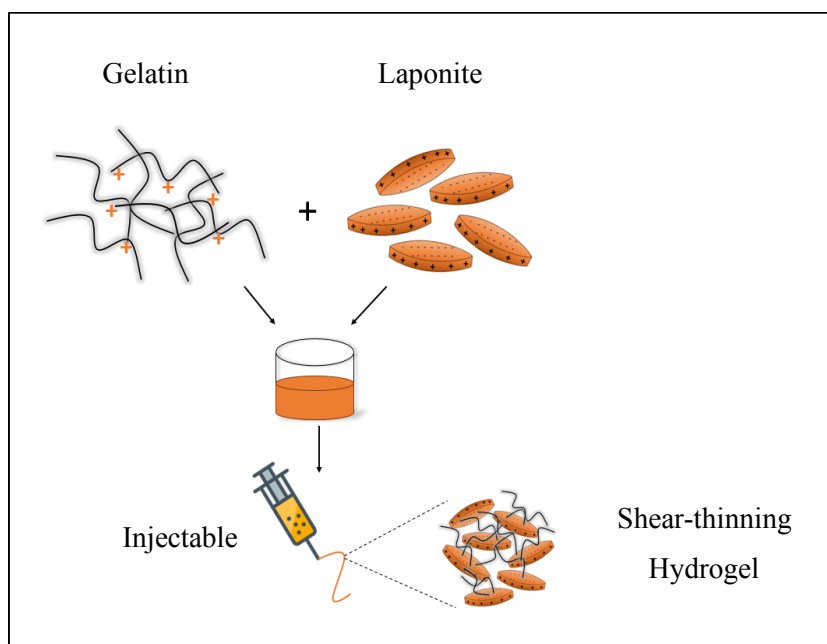


**Figure 5** - Schematic representation of the shear-thinning hydrogel from the mix of gelatin with laponite.

---

<sup>4</sup> Gelatin from porcine source Type A; 300 g Bloom, Sigma Aldrich.



### 2.1.1 Functionalization

The doxorubicin<sup>5</sup> (DOX) is one of the most widely used anticancer drug. It is used for the treatment of various types of cancer, including the hepatocellular carcinoma. The therapeutic behavior of the DOX consists in the intercalation between the adjacent base pairs of the DNA double helix and in the binding with the DNA associated enzymes. Some of the enzymes with which it interacts are the topoisomerase I and II, which lead to a range of cytotoxic effects in conjunction with anti-proliferation, damaging the DNA. It is also known that the DOX interacts with both, DNA and RNA polymerase, blocking the DNA replication and RNA transcription. Additionally, DOX can generate free radicals, causing further damage to the DNA [21]. However, DOX has some side effects, the main one is its cytotoxicity, that can affect many other parts of the body since the DOX itself is not specifically targeted to the tumor. It is also necessary a high dosage of drug to maintain the needed therapeutic level of DOX, due to the drug resistance developed from the body over time which consists in a low efficiency of the drug itself. The functionalization of the STB with the DOX would overcome these side effects since, in this way, the drug is released inside of the tumor tissues in a controlled manner. Thus, it results in an improved efficiency and reduced side effects, due to the decreased amount of drug needed to achieve the therapeutic effect. The DOX, a cationic drug, is encapsulated in the laponite interlayers space and outer surfaces through electrostatic interactions (*figure 6*) [22]. The efficiency of DOX released from the laponite was tested and then compared with the release from the STB loaded with DOX.

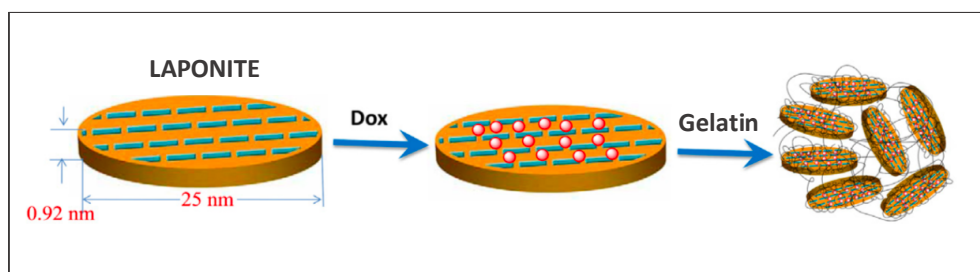


**Figure 6** - Functionalization of the laponite and the final STB with the doxorubicin (DOX).

<sup>5</sup> Doxorubicin hydrochloride (empirical formula (Hill Notation):  $C_{27}H_{29}NO_{11} \cdot HCl$ , molecular weight 579.98), 98.0-102.0% (HPLC), D1515 SIGMA, SIGMA-ALDRICH®.

Furthermore, in order to obtain a more controlled release, it was explored the possibility to load the DOX within disulfide-based mesoporous silica nanoparticles (MSN) dispersed in the STB. Moreover, the MSN are redox responsive mesoporous nanoparticles, since contain disulfide bridges in their framework, thus they are characterized by the ability of a structural degradation when exposed to a reducing agent. This reducing environment can be found inside the cancer cells, therefore the loading of this particles with DOX would increase the local release into the tumor. The MSN used were kindly donated by the *Institute de Science at d'Ingénierie Supramoléculatied (ISIS)*<sup>6</sup>. They are characterized by a spherical shape with a diameter of 100 nm. The pore diameter is around 2.3 nm, sufficiently wide to host the DOX with which can electrostatically interact due to their net negative charge, demonstrated by a Z-potential of around -13 mV (figure 7).

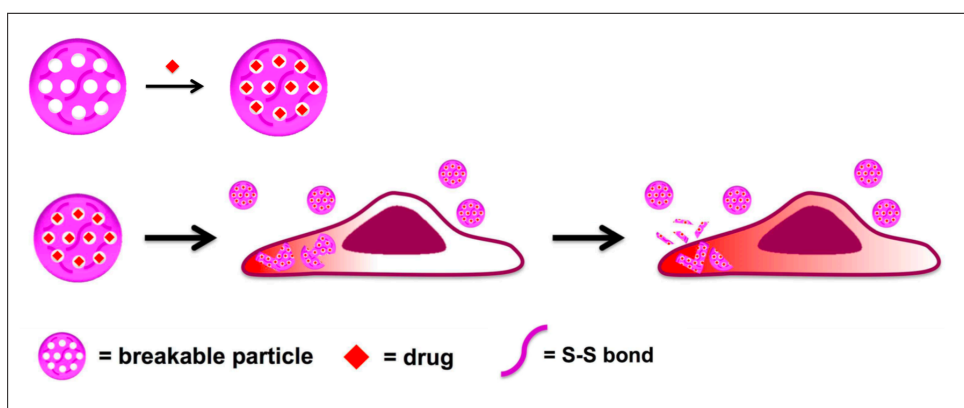


**Figure 7** - Functionalization of the MSN with the DOX and break down of the MSN particles when are in contact with the tumor cell.

<sup>6</sup> Laboratoire de Chimie et de Biomatériaux Speramoléculaires, *Institute de Science at d'Ingénierie Supramoléculatied (ISIS)*, Strasbourg (FR).

## 2.2 Shear-thinning biomaterial preparation

In order to optimize the properties of the STB, different compositions were tested. The various compositions of the STB have been labeled as  $x\text{NC}y$ , where the NC stands for nanoclay, the  $x$  represents the percentage of total solid weight, while the  $y$  stands for the percentage of the solid weight made up of nanoplates. It has been already tested that the best ratio for our purposes are represented by 4NC75, 5NC75 and 6NC75. For this reason, there were analyzed the properties and it was tried to optimize the protocol of the material in these three compositions. For all of them, the preparation of the stock solution of both, the laponite and gelatin, are the same.

The 9% (w/v) Nanoclay stock solution is prepared by using the Laponite XLG-XR, purchased from BYK Additives Inc. The stock solution is obtained by putting 25 ml of milli-Q water<sup>7</sup> in a 50 ml falcon tube<sup>8</sup>, the water is cool down by leaving it in the ice for at least 10 minutes. After that, 2.25 g of laponite powder are added<sup>9</sup> to the cold milli-Q water (4°C) and mixed for 15 minutes using a vortex. The cold water is necessary to prevent the formation of clump of laponite that cannot be dissolved, it retards the gelation allowing the fully dissolution of the nanoplates before gelling. The speed of the vortex<sup>10</sup>, used for mixing the solution, should be of 3200 rpm. The final result is the formation of a transparent shear-thinning gel that have to be stored at room temperature before further use (*figure 9*).

The 18% (w/v) gelatin stock solution is obtained by adding 1.8 g of gelatin powder to 10 ml of milli-Q water, using a 50 ml falcon tube as a container. The solution is mixed for 10 seconds at 3200 rpm and then stored at 80°C for 1 hour, in order to obtain a homogeneous golden colored solution. Afterwards, it has to be

---

<sup>7</sup> Milli-Q water is an ultrapure water obtained with Milli-Q academic water purification system, using a conductivity < 0.06  $\mu\text{S}/\text{cm}$ .

<sup>8</sup> Falcon™ 50mL Conical Centrifuge Tubes, Fisher Scientific.

<sup>9</sup> Weighed through a AL54 Analytical Balance, MATTler TOLEDO.

<sup>10</sup> Fisherbrand™ Analog Vortex Mixer with tube holder, Variable speed: 300 to 3200rpm, Fisher Scientific.

stored in a water bath at 45°C in order to maintain its fluidity. Storing the solution at a lower temperature would make it more solid, whereas the use of a temperature above 50°C for a long period of time would degrade the gelatin.

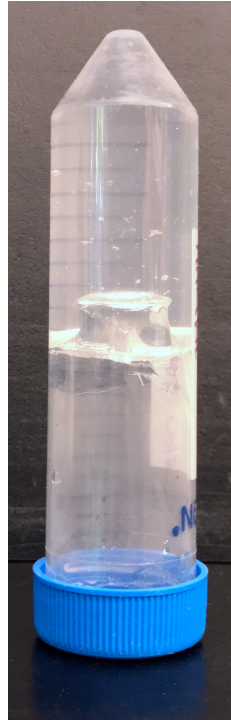


*Figure 8 - Final Laponite transparent gel.*

The STB is realized by mixing the laponite and gelatin stock solutions with milli-Q water, but the ratio and order of the added elements are different depending on the composition of the desired material.

The procedure to obtain the 6NC75 is the following. The first step consists in taking 1.8 g of gelatin from the stock solution, stored in the water bath, and transferring it in a new 50 ml falcon tube. The second component to be added is 10.8 g of nanoclay from the stock solution, which should not touch the gelatin before adding the water, otherwise it would start to cool it down. The last step consists in adding 9 g of milli-Q water. Everything must be done at room temperature and the whole process should take no more than 2 minutes, or the gelatin would start to solidify resulting in a non-homogeneous final material. As soon as all the elements are assembled, they have to be mixed with a speed of 3200 rpm for 15 minutes. After the first 15 seconds of mixing, the mixer has to be

stopped, and the hydrogel mixed with a spatula for a few seconds in order to take all the material components together, also the portion that is attached to the wall of the falcon tube. The hydrogel is then incubated for 10 minutes in the water bath at 45°C to promote the interactions between gelatin and laponite. The final result is a sticky white gel (*figure 10*). The material need to be stored at room temperature for at list 1 hour before further use, in order to cool it down the and stronger the interactions.



*Figure 9 - Final 6NC75, whit in color and sticky to the wall of the falcon tube.*

The 5NC75 and the 4NC75 have the same protocol but distinguished from the use of different ratio. For both of them the first step consists in transferring 9 g of nanoclay inside of a new 50 ml falcon tube. Then the milli-Q water is added in different ratio, 11.5 g for the 5NC75 and 16.5 g for the 4NC75. The solution has to be mixed, with a speed of 2800 rpm, for 4 minutes. After the first 2 minutes the mixer is stopped, and the solution is mixed for 10 seconds with the spatula in order to take and mix all the components together. Afterward, for either the 4NC75 and the 5NC75, 1.5 g of gelatin is taken from the stock solution in the water bath and

added to the prepared solution of laponite and milli-Q water, that has to be immediately mixed for 7 minutes with the vortex. This step should take no longer than 2 minutes in order to obtain a homogenous solution. In this protocol also, after the first 15 seconds, the mixer is stopped and the material is mixed for few seconds with the spatula to incorporate all the elements. The final result is a homogeneous, white, sticky hydrogel. Before further use the hydrogel should stay at room temperature for at least 1 hour. It was noticed how, by increasing the total solid weight, the material became denser and when is injected can form a standing structure. In all the three preparations, during the mixing time, the falcon tube should be hold upright and not move as shown in the *figure 10*.



*Figure 10 - Position of the material on the vortex.*

### 2.3 Material reproducibility

The quality of the material was evaluated by the measurement of the injection force, as well as by the visual appearance, such as the color and the behavior of the material after the gelation. The measurement of the injection force provides an indication about the force required to inject the material, using a 3 ml syringe<sup>11</sup>, in a 5 F catheter<sup>12</sup> with a length of 65 cm. It is also useful to understand if the material is homogeneous or not since the measure is highly sensible to the material composition. The measurement of the injection force should be done within 24 hours after the production of the material, otherwise it would be not representative since it could change over time.

In order to measure the injection force, the cooled down material was transferred with a spatula in a 5 ml syringe<sup>13</sup>. The material was then slowly injected in a 3 ml syringe which was shaken to collect all the material on the bottom part and remove all the bubbles. The syringe should be filled up to the 2.5 ml mark. Afterwards, the syringe was connected to a 5 F catheter and positioned on the Instron<sup>14</sup> mechanical apparatus as shown in the *figure 11*. The end of the catheter was hanging free without touching anything, otherwise it may disturb the measurement of the injection force. It was used a 100 N load cell, since it was comparable with the injection force of the materials, and the Instron was set in a compression force setup. The measurements were recorded with Bluehill 3 software in which there were imposed the diameter of the syringe as 7.2 mm and the flow rate as 33.99 mm/min in order to be comparable with the injection that could applied by hand using a 3 ml syringe. The measurements were repeated three times for each material, to ensure the reproducibility of the measurement itself. The raw data were then represented as shown in the *figure 12*. It is possible to notice an initial increasing of the force which then slowly reaches a plateau. The initial high value

---

<sup>11</sup> BD 3 ml Disposable Syringe with Luer-Lok™ Tips, Fisher scientific.

<sup>12</sup> 5-French Soft-Vu®, 0.038" I.D., Shepherd Hook, AngioDynamics®.

<sup>13</sup> BD 5 ml Disposable Syringe with Luer-Lok™ Tips, Fisher scientific.

<sup>14</sup> INSTRON® Calibration Laboratory, 5943, System ID: 5943S2760.

is representative of the force needed to let the material starts moving in a 5 F catheter with a length of 65 cm, using a flow rate of 33.9 mm/min. Whereas, the value of the plateau is representative of the constant force necessary to keep the material moving through it. The homogeneity of the hydrogel is reflected in a smoothed plateau, otherwise there are several clearly visible fluctuations representative of the different viscosity within the material.



*Figure 11 - Setup of the Instron to measure the injection force of the material.*

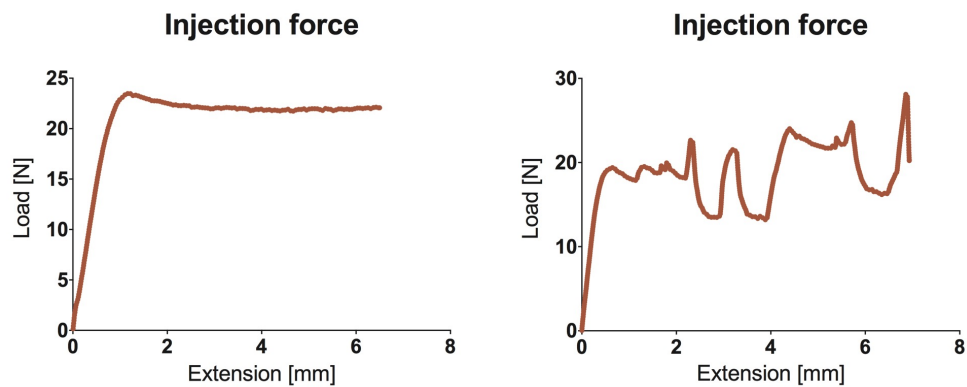


*Figure 12 - On the left it is represented the injection force of a homogeneous material, whereas on the right it is represented the injection force of a non-homogeneous one.*



These measurements were done for all the three material compositions to test their reproducibility. For all of them the results show that, using the described protocols for their preparation, it is possible to reproduce them homogeneously. For each composition there were produced more than one batch of material to demonstrate their reproducibility. Each material produced was tested three times with the measurement of the injection force to make the measure more consistent. For each composition the mean of three measurements of the injection force was reported in a bar graph with the relative standard deviation. The 4NC75 showed to have an injection force of  $4\pm 2$  N for all the materials produced. With the same procedure it was shown that the 5NC75 has an injection force of  $8\pm 2$  N, whereas the 6NC75 has an injection force of  $22\pm 2$  N (*figure 13*).

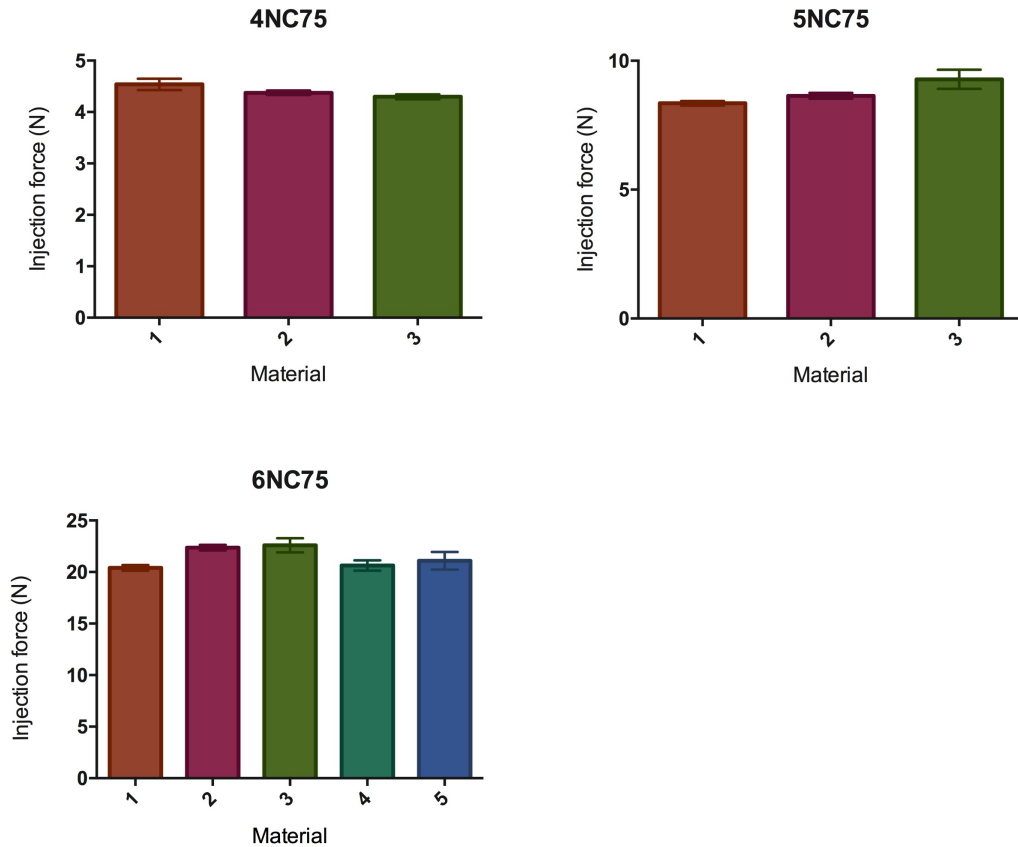


**Figure 13** - There are represented the bar graphs of the injection force of the 6NC75, the 5NC75 and the 4NC75 with the respective standard deviations. It is possible to observe the value of the injection force and to notice the reproducibility of all the three compositions.

## 2.4 Material optimization

In order to optimize the reproducibility of the material, different changes were made on the protocol. It is known that the behavior of both, laponite and gelatin, is strictly dependent on the temperature and mixing time. The procedure to obtain the 6NC75 was the only one tested, its protocol was modified with four different adjustments. As it was mentioned, the gelatin is highly sensible to the temperature so, during the time in which the elements are added together, if the temperature decrease, the gelatin could cool down and solidify. The result would be a non-homogeneous material since there would have been not enough interactions between gelatin and laponite before the gelation. In order to prevent it, it was tested the same protocol but changing the temperature of the milli-Q water. The tested procedures are described below.

The milli-Q water was incubated in the water bath at 45 °C, together with the gelatin, in order to maintain them at the same temperature until they would be further mixed. However, the laponite is sensitive to the temperature too and the use of a warm milli-Q water would produce aggregations in the laponite. Using the same ratio of the original protocol for the 6NC75, the gelatin was transferred from the water bath in a new 50 ml falcon tube. Thereafter, the correspondent ratio of nanoclay was taken from the stock solution and the last component to be added was the warm milli-Q water. Everything was done in a few minutes and immediately mixed for 15 minutes at room temperature, using a speed of 3200 rpm. After the first 15 seconds, the solution was manually mixed with the spatula for a few seconds, in order to take all the components together. The hydrogel was then incubated in the water bath at 45 °C for 10 minutes and after that it was stored for 1 hour at room temperature before measure the injection force. This procedure was tested for seven times. The final materials were quite homogeneous, as it is shown in the graphs of the injection forces of the materials tested (*figure 14*). Although, they were non-reproducible, since the injection forces of the different samples tested were highly different (*figure 15*). Moreover, from a visual analysis the hydrogel, represented in the *figure 16*, results more transparent, softer and not enough sticky compared to the desired material produced with the standard protocol

and represented in the *figure 9*. Thus, the viscoelastic properties of the material were affected by the temperature, generating different interactions.

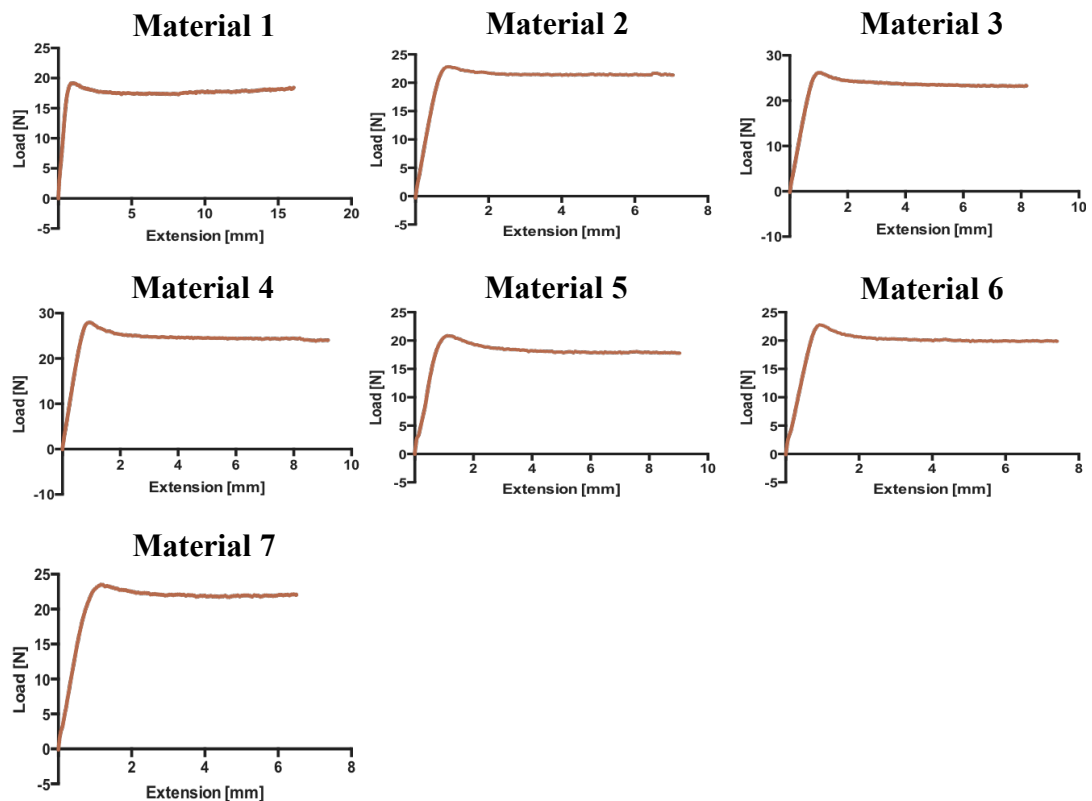


**Figure 14** - Representation of the injection force of seven materials tested using a warm milli-Q in the protocol for the 6NC75. In all the graphs it is observable a flat plateau, characteristic of a homogeneous material.

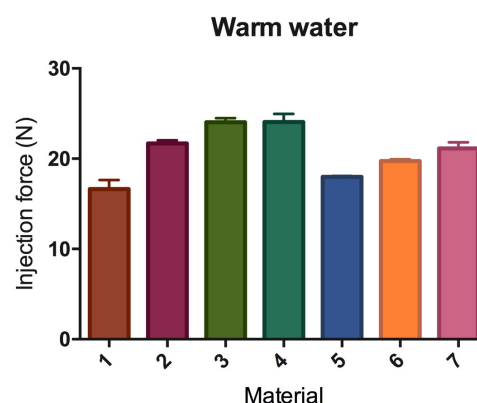


**Figure 15** - Bar graph to compare the values of the injection forces of the different materials tested using the warm milli-Q water in the protocol. It can be seen that the values of the injection forces are highly different between the tested materials, highlighting the non-reproducibility of this method.

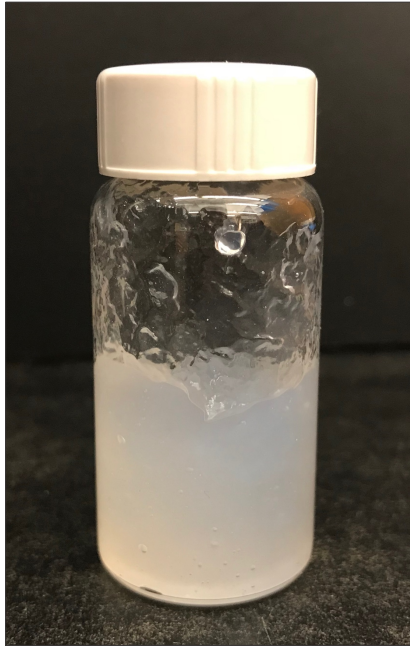


*Figure 16 - 6NC75 made with warm milli-Q water. It is possible to see a more transparent aspect compared to the material produced with the standard protocol and showed in the figure 9.*

Since the obtained materials were non-reproducible and their properties did not represent the required 6NC75, another experiment was performed. It was tried to use the cold milli-Q water instead of the warm one, because the laponite is also affected by the temperature of the water. The milli-Q water was incubated in an ice bath at 4 °C. The components were added together with the same ratio and order of the original protocol of the 6NC75, mixed for 15 minutes with the vortex at 3200 rpm and with a spatula for some seconds after the first 15 seconds. The material was then incubated at 45 °C for 10 minutes and, after 1 hour of rest, it was tested with the measurement of the injection force. This procedure was applied three times. The results were non-homogeneous materials, as it is shown in the graphs of their injection force, in which instead of a flat plateau multiple bumps are clearly visible (*figure 16*). It may be possible because, as soon as the cold water went in contact with the gelatin, this became more solid and did not leave the time to generate all the bonds between the gelatin and the laponite, hindering the hydrogel formation. Moreover, the values reached from the injection forces were highly different among the tested materials, showing a non-reproducibility of the 6NC75 using this protocol (*figure 17*). From a visual analysis, the materials showed their

non-homogeneity from the color as well as they seemed to be less sticky, therefore more viscous but less elastic than the desired 6NC75.

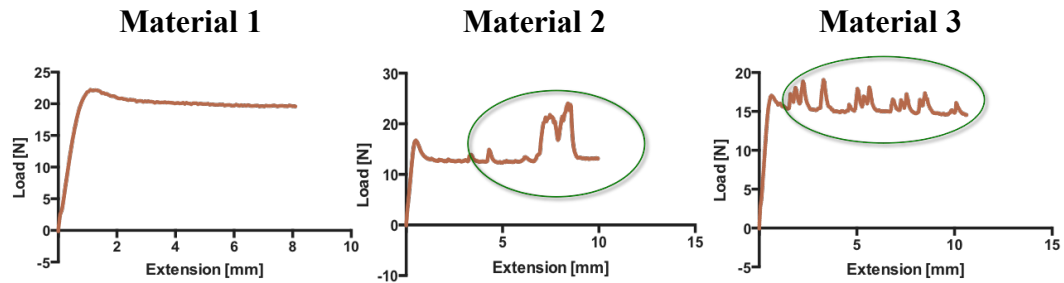


**Figure 17** – Representation of the injection forces of the three materials tested using a cold water in the protocol of the 6NC75. In the graphs of the material 2 and 3, it is clearly visible the presence of bumps, which represent the non-homogeneity of the materials.

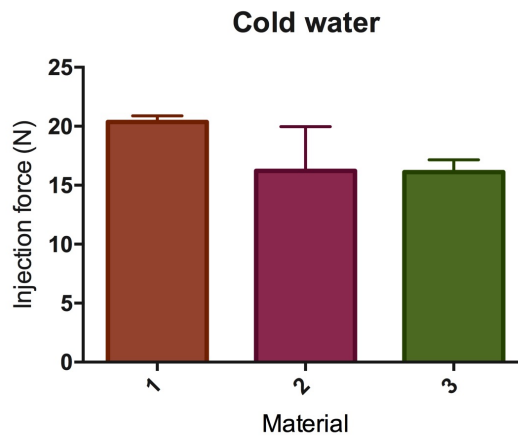


**Figure 18** – Representation in a bar graph of the injection forces of the three materials tested using the cold water in the protocol of the 6NC75. It can be observed that the values of the injection forces are highly different between the tested materials, highlighting the non-reproducibility of this method.

In order to build stronger interactions within the material, it has been tried to increase the mixing time up to 3 hours. The experiment was performed as is fallowing explained. The gelatin, laponite and milli-Q were taken from the respectively stock solutions and added together at room temperature, with the same ratio an order of the original protocol of the 6NC75. The material was mixed using a vortex with a speed of 3200 rpm for 3 hours at room temperature. After the first

30 seconds, it was mixed with the spatula for other 30 seconds, just to ensure the mixing of all the components inside of the falcon tube. The material was then left on the vortex, and after each hour, it was mixed for 5 minutes with the spatula and then put back on the vortex. Thus, this procedure of mixing the material with the spatula, was repeated for three times and after each hour the temperature was measured. The temperature was evaluated to be respectively of 45 °C, 44 °C and 43 °C after 1 hour, 2 hours and 3 hours of mixing. The hydrogel was then incubated for 10 minutes in the water bath at 45 °C. The result, after 1 hour of incubation at room temperature, was a phase separated gel, the gelatin and the laponite were not well incorporated, and the material was not sticky (*figure 23, I*). The hydrogel was tried to be made with this method for three times and tested with the measurement of the injection force. As it is clearly shown in the *figure 19*, the graphs of the injection forces present numerous bumps for all of the materials that were tested, which represent the non-homogeneity of the materials. Moreover, the hydrogel was not reproducible with this method since each material that was produced presented a different value of the injection force (*figure20*). The materials were also tested to be injected by hand through a 32 G needle using a 5 ml syringe, showing the different consistence of these materials from the good 6NC75 obtained with the standard protocol. They spread out when were injected, while the good one used to build a standing structure (*figure 24*). It is possible that the problem was the increasing of the temperature, which reached a very high level for almost all the time of the procedure.

In order to contrast the high temperature reached during the mixing time, a new experiment was performed inside of a cold room at the temperature of 4°C. The procedure was the same of the previous experiment, with the only difference in the performing temperature (4 °C). Thus, the components were added together in the order and amount of the original protocol for the 6NC75. The material was mixed for 3 hours inside of the cold room at 4 °C, after the first 15 seconds it was mixed by hand for a few seconds and, after each hour, it was mixed for 5 minutes with the spatula. The material was monitored, and after 1 hour, 2 hours and 3 hours the temperature was respectively of 22 °C, 21 °C and 20 °C. The material was then incubated in a water bath at 45 °C for 10 minutes. Even if the material was almost

at room temperature for all the mixing time, the final result was visually different from the original 6NC75. The hydrogel was more transparent and soft, it had the same problem of the material produced at room temperature with a long mixing time (*figure 23, II*).

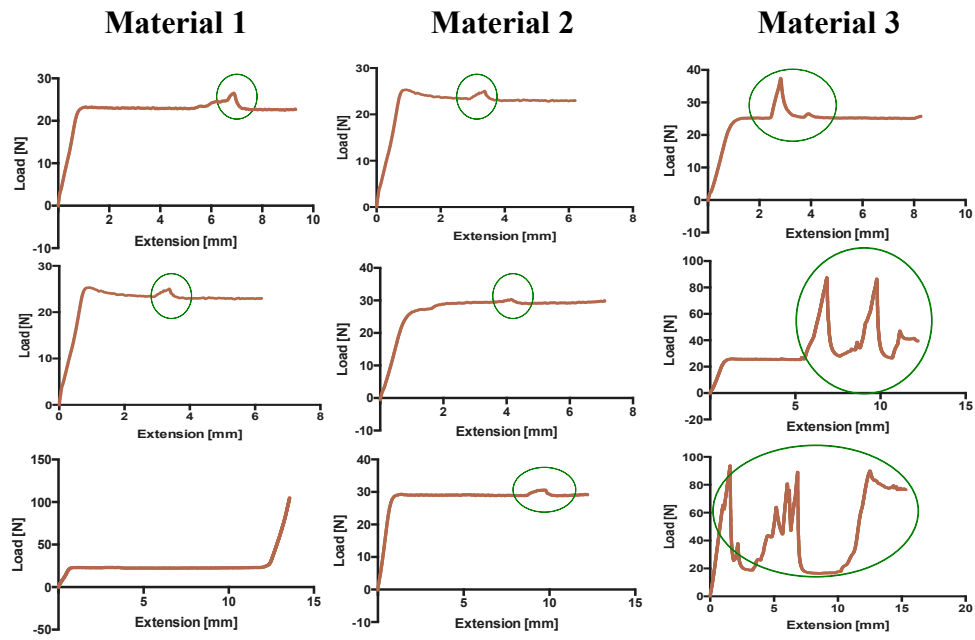


**Figure 19** - Representation of the injection forces of the 6NC75 realized with 3 hours of mixing at room temperature. For each material the measurement was repeated three times. It is clearly visible the non-homogeneity of the materials.

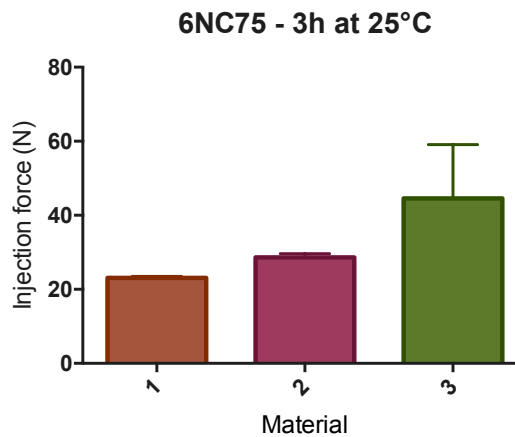


**Figure 20** – There are compared, in a bar graph, the injection forces of the three materials made with 3 hours of mixing at room temperature. It is observable the non-reproducibility of the material using this method.

As for the previous experiment, three materials were made with this protocol and tested with the measurement of the injection force after 1 hour of resting at room temperature. All the materials tested presented a fluctuating injection force, representative of a non-homogeneity (*figure 21*). Moreover, comparing the values of the injection forces, they were very different each other demonstrating a non-reproducibility of this protocol (*figure 22*). The materials obtained with this method were also tried to be injected by hand through a 32 G needle. When they were injected they spread out, instead of building a standing structure, demonstrating a different viscosity and elasticity from the good 6NC75 (*figure 24*).

It is possible that the increasing of the mixing time had destroyed the bonds between the laponite and gelatin. The effect of the temperature and the mixing time are both very important and the best combination seems to be the one already used in the original protocol described in the chapter 2.2.

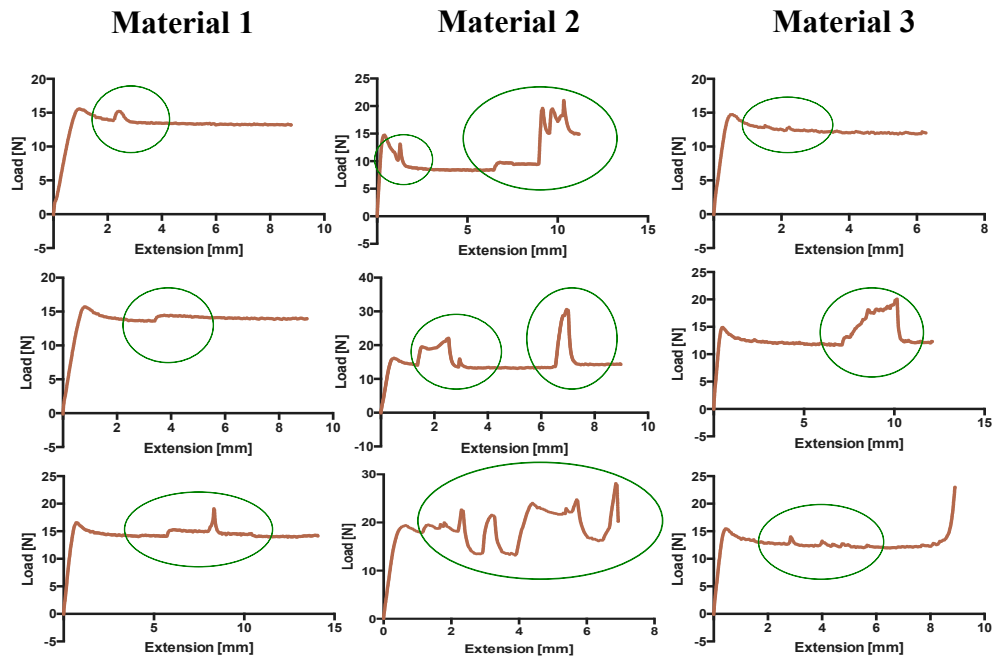


**Figure 21-** Representation of the injection force of the 6NC75 realized with a mixing time of 3 hours performed in the cold room (4°C). Each measurement was repeated three times to be consistent. The results show numerous bumps in the graph, synonymous of the non-homogeneity of the materials.



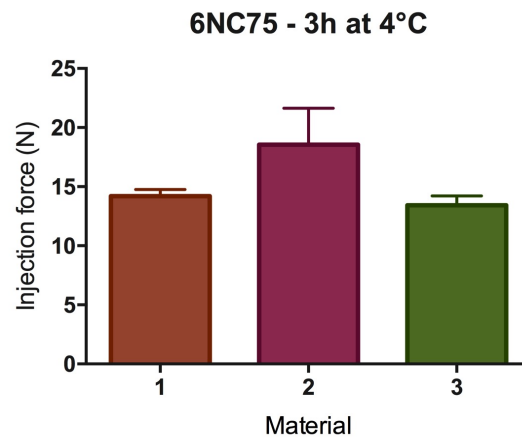


**Figure 22** – Bar graph of the injection forces of the 6NC75 realized with 3 hours of mix in the cold room (4 °C). It shows a difference between the injection forces of the three materials tested, representing a non-reproducibility of the 6NC75 using this method.

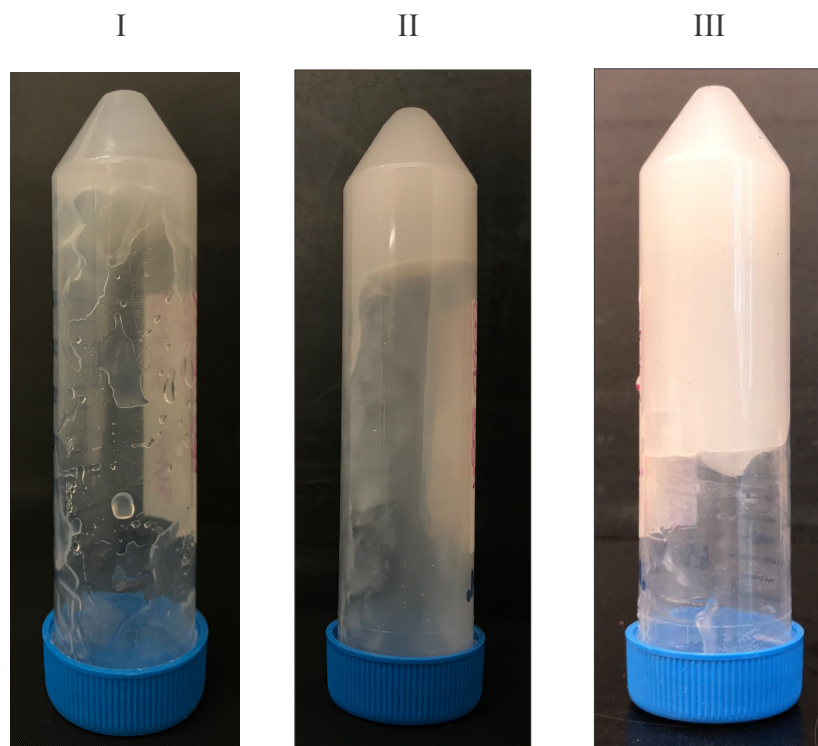
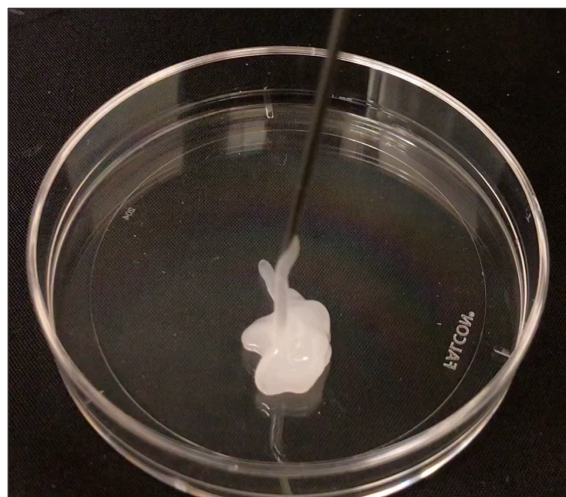
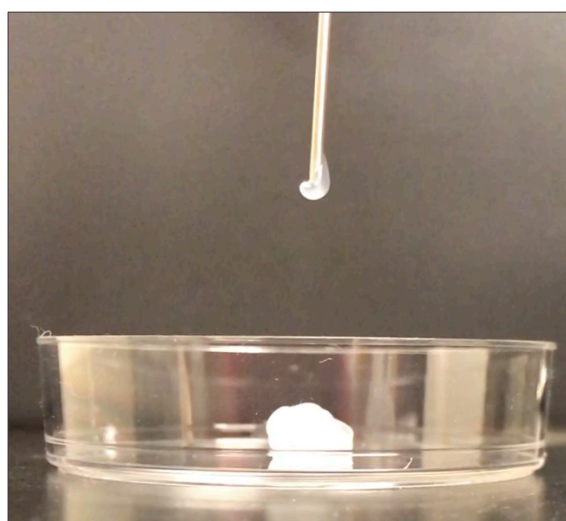


**Figure 23** - A comparison between the 6NC75 realized with 3 hours of mixing time at 21°C (I), 3 hours of mixing time at 4°C (II) and the material realized using the standard protocol (III).

I)



II)



III)

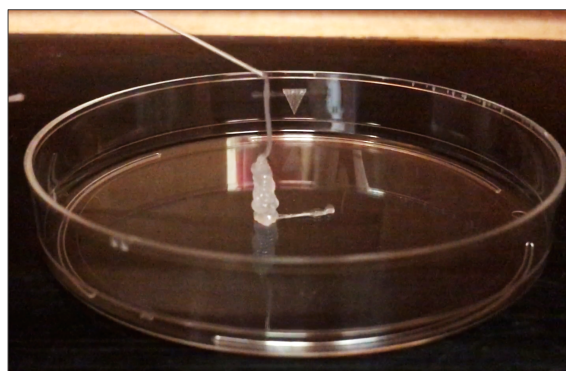


**Figure 24** - Comparison between the injected 6NC75 realized with 3 hours of mixing at 21°C (I), 3 hours of mixing at 4°C (II) and with the standard protocol (III). It is visible how the material I and II spread out when injected, whereas the III is able to form a standing structure.

### **3 In vitro characterization**

The three shear-thinning biomaterials, that were realized using different ratio, 6NC75, 5NC75 and 4NC75, were mechanically characterized with multiple in vitro experiments. First of all, it was evaluated the possibility to inject the materials through different sizes micro tubes, in order to demonstrate their potential employment in the micro vasculature of the tumor. It was also evaluated the degradation of the materials into solid components, that would be released inside of the circulation. Even if the degradation products of the studied STB are biocompatible, it would be better if the materials would maintain their composition when are in loco. Therefore, it was studied the possibility of the materials to absorb or release fluids once injected inside of the body, a feature that would compromise the shape and behavior of the materials when are placed in the tumor vascularization. Moreover, it was analyzed the behavior of the materials when stored for a long period of time, under different environment conditions. Finally, it was tested the ability of the materials to occlude different sizes micro tubes under the systolic pressure, to show their potential to occlude the microvasculature of the tumor.

#### **3.1 Injectability**

One of the most important feature of the STB, in order to be used for the chemoembolization of a tumor, is its ability to be injected inside of the micro vasculature of the tumor, with the aim of blocking its feeding and avoid its revascularization. This property was evaluated as it is following described.

The three compositions of the material were tried to be injected by hand in PEEK micro tubes<sup>15</sup> having a diameter comparable with the microvasculature of the tumor. There were used the PEEK micro tubes since this is one of the best material that can be used in order to simulate the friction coefficient of the

---

<sup>15</sup> PEEK tubing natural; Outer diameter: 360µm; inner diameter: 25 µm, 50 µm, 100 µm, 150 µm, 300 µm, IDEX Health & Science.

vasculature. Indeed, the friction coefficient of the PEEK is around 0.3, whereas the friction coefficient of the endothelial cells is between 0.03 and 0.1. The endothelial one is much lower, but it is difficult to find tubes that better mimic this property [22]. Everything was done at room temperature (21°C). There were used a 300  $\mu\text{m}$ , 150  $\mu\text{m}$ , 100  $\mu\text{m}$  and 50  $\mu\text{m}$  tubes, each one with a length of 3.5 cm. It was found out that the 4NC75, the softest of the three compositions, resulted easily injectable in all the micro tubes. Whereas, the 5NC75 was easily injectable in all of them except for the smallest tube (50  $\mu\text{m}$ ), in which it was still injectable but in a hardly way. Finally, the 6NC75 was completely not injectable in the 50  $\mu\text{m}$  tube but it could be easily injected in the other size micro tubes (*figure 25*). In the *figure 26* it is shown the difference between the 4NC75, 5NC75 and 6NC75 injected through a 100  $\mu\text{m}$  tube<sup>16</sup>. It is clearly visible that, increasing the percentage of solid particle, the material become less liquid and more viscous, able to form a standing structure.

Material composition \ Inner diameter ( $\mu\text{m}$ )						
	50	100	150	300	✓	Easily injectable
4NC75	✓	✓	✓	✓	≡	Hardly injectable
5NC75	≡	✓	✓	✓	X	Not injectable
6NC75	X	✓	✓	✓		

*Figure 25 - Summary of the injectability of the materials through micro tubes with different inner diameter.*

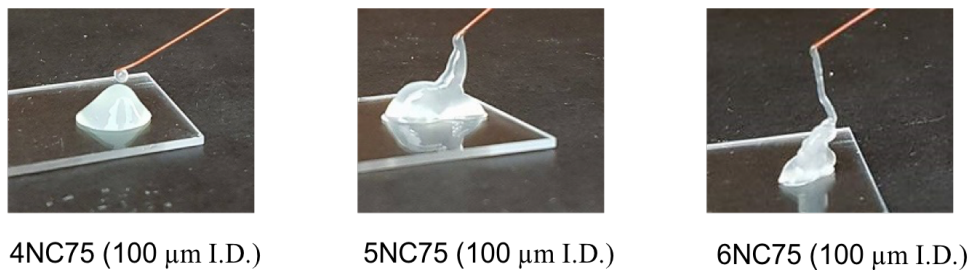


*Figure 26 - Comparison between the three different compositions of the material injected through micro tubes with an inner diameter of 100  $\mu\text{m}$ .*

<sup>16</sup> These results were achieved in collaboration with my colleague Edoardo Cuniberto.

### 3.2 Degradation

In order to study the possible degradation of the material, its behavior was analyzed in conditions that simulate the environment inside of the body. The potential degradation of the STB would consist in a loss of solid particles which, even if would not be toxic, could generate a loss of the material's ability to block the flow in the blood vessels, due to a change in its shape and composition. The STB was tested in all the three compositions, 4NC75, 5NC75 and 6NC75. The experiment was conducted in the following way.

For each composition, the material was prepared three times and, for each material prepared, there were taken three samples. In the end there were a total of nine samples for each composition of the STB. Moreover, the nine samples that represent the single material were prepared for each time point. The time points were decided to be set at 0,1,2,4,8,24 hours, 3,7,14,30 days. Each sample was prepared by filling, through the use of a 5 ml syringe, a pre-weighed 2 ml Eppendorf<sup>17</sup> with 1 g of material. The samples were then centrifuged, with a mini centrifuge<sup>18</sup>, to obtain a flat surface and collect all the material on the bottom of the Eppendorf. The Eppendorf with the material was weighed again in order to obtain, by subtraction, the weight of the material. Each sample was covered with 500 µl of a phosphate buffer saline solution (PBS)<sup>19</sup>, in order to simulate the body fluid with which it should be in contact during the occlusion of the vessel. The samples were then stored in the incubator at 37 °C. At each time point the corresponding sample was cleared from the PBS, paying attention to not touch the material surface, and frozen at -80 °C. The samples were freeze dried, to take off all the liquid components, and weighed, after the freeze drying, in order to know the percentage of solid components present in each sample. The time point zero was represented

---

<sup>17</sup> 2 ml Eppendorf™ Snap-Cap Microcentrifuge Safe-Lock™ Tubes, Polypropylene tube with locking cap, Fisher (05-402-7).

<sup>18</sup> Mini Centrifuge, power 115-240 Volt 50/60 Hz, Max. speed/force: 6600rpm/2200xG, Capacity: 0.2mL, Fisher Scientific (05-090-100).

<sup>19</sup> Dulbecco's Phosphate-Buffered Saline (DPBS) powder (Fisher scientific) was mixed in 1L of DI water (pH 7.4, 0.15M).

by a sample that was not stored with the PBS but immediately freeze dried and used as a referent, for the correspondent bunch of material, of the initial content of solid particles. The percentage of solid content of the sample at each time point was evaluated with the following formulas.

$$\text{Solid content (Sc)} = \frac{w_{fdm}}{w_m} \quad (1)$$

$$\text{Initial solid content (Sc}_i\text{)} = \frac{w_{fdm_0}}{w_{m_0}} \quad (2)$$

$$\text{Solid content \%} = \frac{Sc}{Sc_i} \times 100 = \frac{(w_{fdm}/w_{fdm_0})}{(w_m/w_{m_0})} \times 100 \quad (3)$$

In the equation (1) is evaluated the solid content ( $Sc$ ) present inside of the sample that is wanted to be measured, in which  $w_{fdm}$  is its weight after it was freeze-dried and  $w_m$  is the weight of the hydrated sample before the freeze-dry procedure. Whereas, in the equation (2) it is calculated the solid content of the respective sample at the time point zero ( $Sc_i$ ). In this equation  $w_{fdm_0}$  and  $w_{m_0}$  are respectively the weight of the freeze dried and hydrated sample at the time point zero. Finally, with the equation (3), it is evaluated the percentage of solid content of the sample, at the determinate time point, normalized by its initial solid content. The initial solid content is considered the same for all the sample from the same bunch of material, because it was not possible to evaluate it for each sample since it means to freeze-dry the sample before starting the incubation time.

The swelling ratio of all the three materials is represented in the *figure 27*. Although the eventually degradation would not be a big problem, since the degradation products of the materials have been previously studied to be not toxic for the body until quite high concentrations, it would be better to not loss any solid component to maintain the materials composition. The results show that, in all the three compositions, the STB can be considered stable in PBS up to 30 days. For all the materials, it is possible to observe an initial bump, maybe due to an initial

absorption of body fluid from the material that would be in accordance with the study of the swelling. Moreover, the percentage of total solid content detected seems to slowly increase, even though the maximum degradation observed is of the order of 5%, comparable to an error of pipetting or of weighing the materials. This means that the STB should not loss solid components, in an environment that simulate the body fluid, up to at least the first month after its injection.

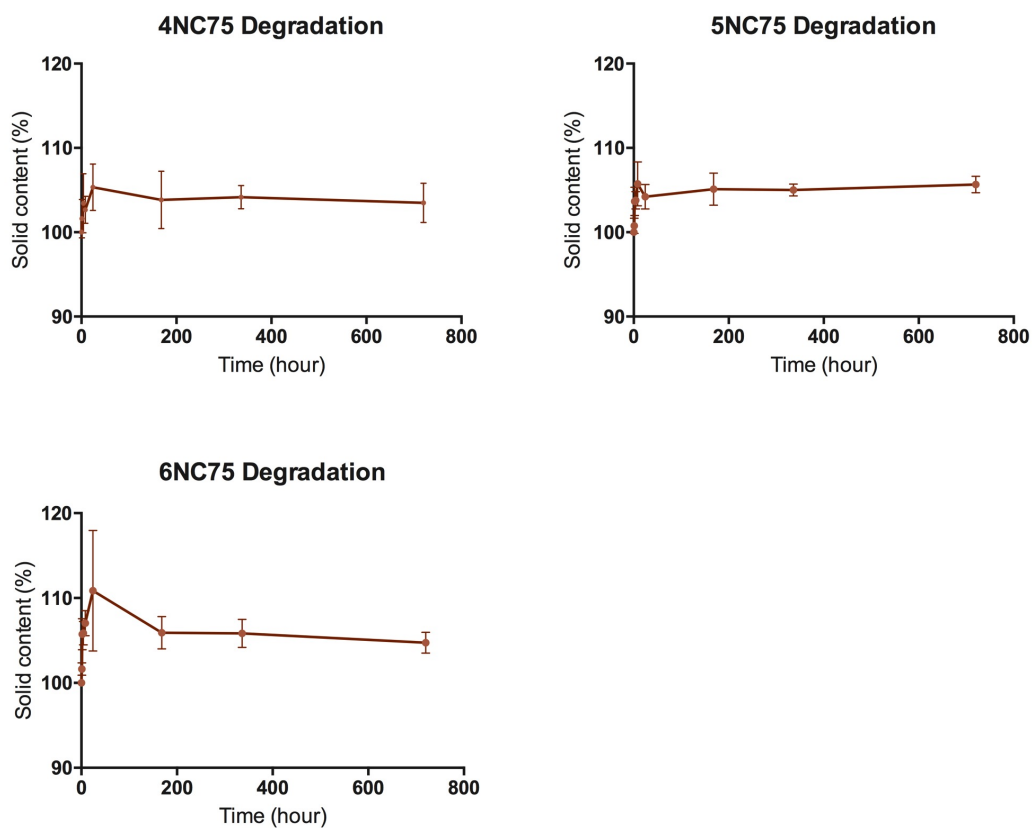


**Figure 27** - Representation, for the 4NC7,5 5NC75 and 6NC75, of the percentage of solid content of the samples, up to one month after their incubation at 37°C in contact with PBS. For each time point it is reported the mean of the values of the solid content of three samples, with the respective standard deviation.

### 3.3 Swelling

The swelling is the capacity of the material to absorb liquid from the environment. It was tested the swelling of the STB for all the three compositions of the material, 4NC75, 5NC75 and 6NC75. Since the aim of the STB is to occlude the micro vasculature of the tumor for a long period of time, it should not swell, because it would consist in an absorption of body fluid or in a release of water in the surrounding environment. The experiment was performed at 37 °C and using a phosphate buffer saline solution (PBS)<sup>20</sup> as supernatant, in order to simulate the physiologic condition. The protocol was the same for all the three compositions of the STB. For all of them, there were tested three different bunches of material and three samples for each bunch. The protocol was designed as follow.

The STB was loaded inside of a 5 ml syringe<sup>21</sup> and 1 g of the material was transferred in a 2 ml Eppendorf<sup>22</sup>. For each sample, the empty Eppendorf was previously weighed and then weighed again with the material inside. It was then centrifuged in a mini-centrifuge<sup>23</sup> for 10 seconds in order to collect all the material on the bottom of the Eppendorf and obtain a flat surface. Afterward, 500 µl of PBS were added over the STB, taking care of pipetting it against the wall of the Eppendorf to prevent the formation of cavity in the sample. The sample was then stored in the incubator at 37°C. After each time point, that was fixed at 1,2,4,8,24 hours, 7,14, 30 days, the PBS was carefully removed from the Eppendorf without touching the material. The sample was weighed again to calculate the ratio of swelling, therefore 500 µl of new PBS were put over the material and the sample was stored until the next time point. The percentage of swelling of the material, was evaluated by normalizing the weight of the material, at the time that is wanted to be

---

<sup>20</sup> Dulbecco's Phosphate-Buffered Saline (DPBS) powder (Fisher scientific) was mixed in 1L of DI water (pH 7.4, 0.15M).

<sup>21</sup> BD Disposable Syringe with Luer-Lok™ Tips, Fisher scientific.

<sup>22</sup> 2 ml Eppendorf™ Snap-Cap Microcentrifuge Safe-Lock™ Tubes, Polypropylene tube with locking cap, Fisher (05-402-7).

<sup>23</sup> Mini Centrifuge, power 115-240 Volt 50/60 Hz, Max. speed/force: 6600rpm/2200xG, Capacity: 0.2mL, Fisher Scientific (05-090-100).



calculated, by its initial weight. The weight of the material is calculated by subtracting the weight of the Eppendorf from the weight of the material and the Eppendorf. The initial weight of the sample was determinate at the time zero, before covering it with the PBS. The formula used was the following.

$$\text{Swelling \%} = \frac{w - w_0}{w_0} \times 100 \quad (4)$$

Where  $w$  is the weight of the sample at the determinate time point, and  $w_0$  is the weight of the sample at the time point zero.

The results, that are represented in the *figure 28*, show that all the three compositions of the STB, besides an initial small bump maybe due to an error of pipetting, do not absorb any liquid. On the other hand, some liquid was probably lost from the samples, resulting in a negative swelling. The 4NC75 present a negative swelling percentage around 10%. Whereas, the percentage of swelling for the 5NC75 and the 6NC75 was negative and less than 5%. In all the cases there were very low swelling percentage if compared with the pipetting error that was estimated to be around 2%. Moreover, the mass loss is highly probable water since, analyzing the data from the degradation experiment, no solid mass was lost during the permanence of the material in the PBS for the same length of time. In the first 8 hours there can be observed a little initial swelling, that is in accord with the results obtained from the degradation but could also be an error since it is less than 3%. These results show a good behavior of all the three materials when are incubated up to one month in an environment that mimics the physiologic one. What emerged is that they do not loss a relevant quantity of mass, neither liquid or solid, and at the same time do not absorb any liquid from the surrounding environment. These results can be reflected in the stability of the materials, that should not loss their properties, once injected in the microvasculature of the tumor.

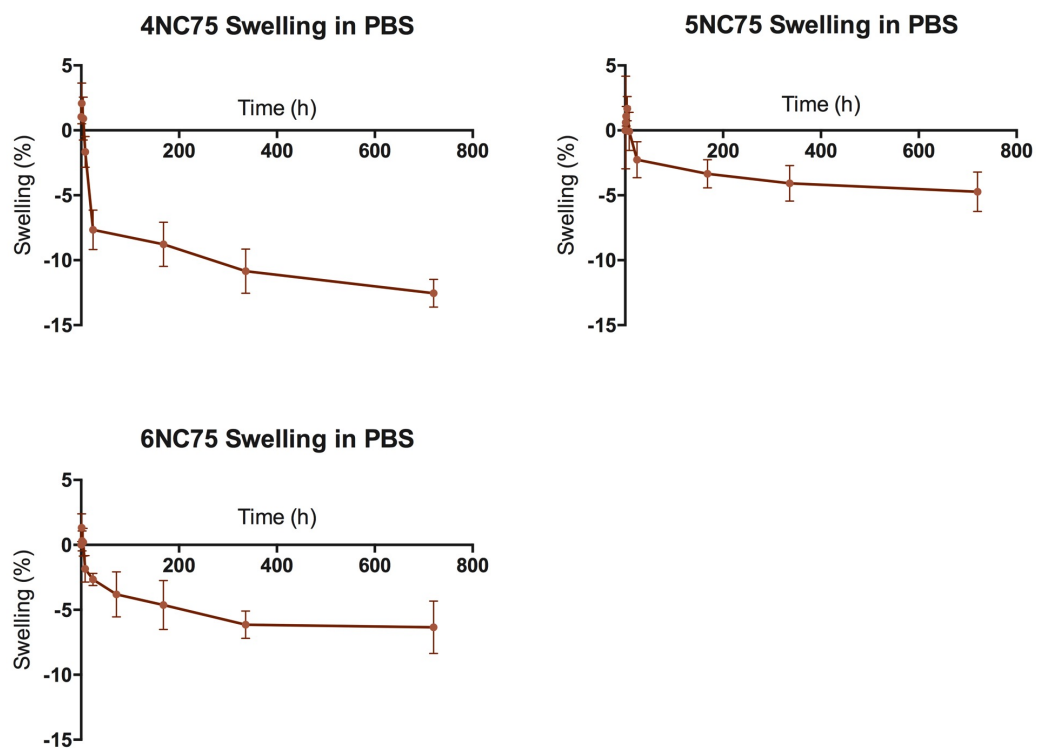


**Figure 28** - Representation of the percentage of swelling for the 4NC75, 5NC75 and 6NC75 when are incubated up to 1 month at 37°C surrounded with PBS.

### 3.4 Shelf life

The shelf life of a material is the length of time that it can be stored without becoming unfit for its use. It is an important parameter in the medical field since most of the materials used cannot be synthesized in the hospital, immediately before their employment. Thus, it is important to analyze the best way to store them for a long period of time. The production of the studied STB is not so easy to be made in a hospital, therefore its shelf life, in all the performed concentrations, was investigated in order to understand if it is a material that can be stored for a great deal of time before its use. There were analyzed which are the best storing conditions, for the studied materials, so that they would maintain their properties. The 4NC75, 5NC75 and 6NC75 were all tested, and, for each composition, different storing conditions were examined. There were performed three different experiments. The materials were tested to be frozen at  $-20\text{ }^{\circ}\text{C}$ , stored at room temperature ( $21\text{ }^{\circ}\text{C}$ ) and stored in a cold room at  $4\text{ }^{\circ}\text{C}$ . It was also tested the possibility to freeze-dry the materials and store them as a powder before their employment. The materials would be then rehydrated only before their use.

For each composition of the STB, there were filled 3 syringes of 3 ml and stored at  $-20\text{ }^{\circ}\text{C}$ . The samples frozen showed, already after 24 hours, a highly phase separation. As it is shown in the *figure 29*, the solid content was completely separated from the liquid one. It was not possible to test them using the measurement of the injection force, since the materials were extremely heterogeneous. As a matter of fact, when they were injected through a syringe, initially only the aqueous component came out and eventually the solid one. Thus, the experiment was not carried on after the first 24 hours. Moreover, it was considered a method that cannot be applied to store the STB.

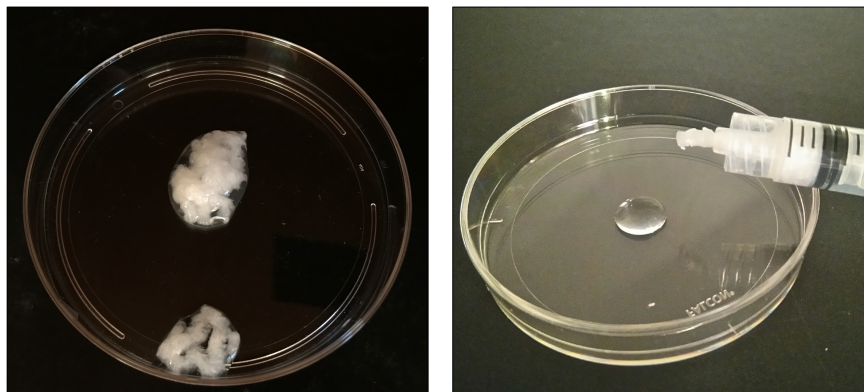


*Figure 29 - It is shown the 4NC75 store for 24 hours at - 20°C. It is possible to see a completely phase separation between the liquid and the solid components of the material.*

The materials were then tested to be stored both, at room temperature (21 °C) and at 4 °C. The two experiments were performed using the same protocol. For each experiment, three different bunches of material were prepared for each STB compositions (4NC75, 5NC75 and 6NC75) and, for each bunch of material prepared, there were loaded 6 syringes<sup>24</sup> of 3 ml. The syringes were filled up to the 2.5 ml ticket and were tightly closed on the top with some Parafilm<sup>25</sup>. Afterwards, they were centrifuged<sup>26</sup> for 5 minutes at 2500 rpm, in order to remove all the possible air bubbles presents in the materials. The syringes were checked to be well closed and stored, depending on the performed experiment, at room temperature (21°C) or at 4°C. Thereafter, at each time point, the samples were characterized by the measurement of the injection force. The time points were decided to be set at time zero, before storing the samples, and after 24 hours, 3,7,14 and 30 days. The samples stored in the cold room were equilibrated at room temperature for 1 hour before any measurements. The results are represented in the *figure 30*. All the materials stored were visibly the same as before the storing time. However, regarding the experiment performed at room temperature (21°C), it was possible to notice a highly increase in the injection force for all the three compositions. It can be interpreted as a changing in the mechanical properties, such as the viscosity and

---

<sup>24</sup> 3 ml BD Disposable Syringe with Luer-Lok™ Tips, Fisher scientific

<sup>25</sup> Bemis™ Parafilm M™ Laboratory Wrapping Film, Fisher scientific.

<sup>26</sup> Sorvall legend RT centrifuge, Thermo Scientific.

elasticity of the materials. After the first 14 days, the injection force seems to stabilize or decreasing, indicating that the materials were subject to an aging process that could slowly reach an equilibrium. The samples stored at 4 °C also showed an increasing injection force with the time, but with a slower rate compared the samples stored at room temperature. Analyzing the single material, it is possible to see how the 4NC75, stored at room temperature (21 °C), showed after 14 days an increasing in the injection force of around 3 N, which tended to reach the initial value of 5 N after 1 month. Whereas, when it was stored at 4 °C the increasing of the injection force was more gradual and reached a maximum of + 2 N after 30 days. A similar behavior can be observed in the 5NC75. When it was stored at 21 °C, its injection force had an initial increase of 4 N after the first 3 days and then came back to the initial value around the 8 N. Furthermore, when it was stored at 4 °C its injection force showed a slower increase till reaching a maximum of + 3 N after 30 days. For what concern the 6NC75, the trend of the injection force is approximately the same of the other two materials, but it showed a higher increase. In fact, when it was stored at 21 °C its injection force reached a maximum of + 15 N after the first 14 days. Whereas, when it was stored at 4 °C the trend was slower, and the injection force was increased of around 8 N. Thus, in all the three materials stored at 21 °C, it is possible to notice a higher increase in the injection force after a shorter period of time and that tend to reach its initial value after 30 days. Whereas, when were stored at 4 °C, the increasing rate of the injection force was slower and also lower. Thus, all the materials seem to be subject to a process of aging that tend to reach an equilibrium, and which is also slow down by the low temperature. Therefore, the low temperature seems to better preserve the original properties of the materials for a longer period of time. However, further studies are necessary to understand the behavior of the materials after more than 30 days and to see if their injection force is going to stabilize with a longer storing time. Moreover, there should be stored a greater quantity of material to study if they will maintain the mechanical properties of the original studied materials.

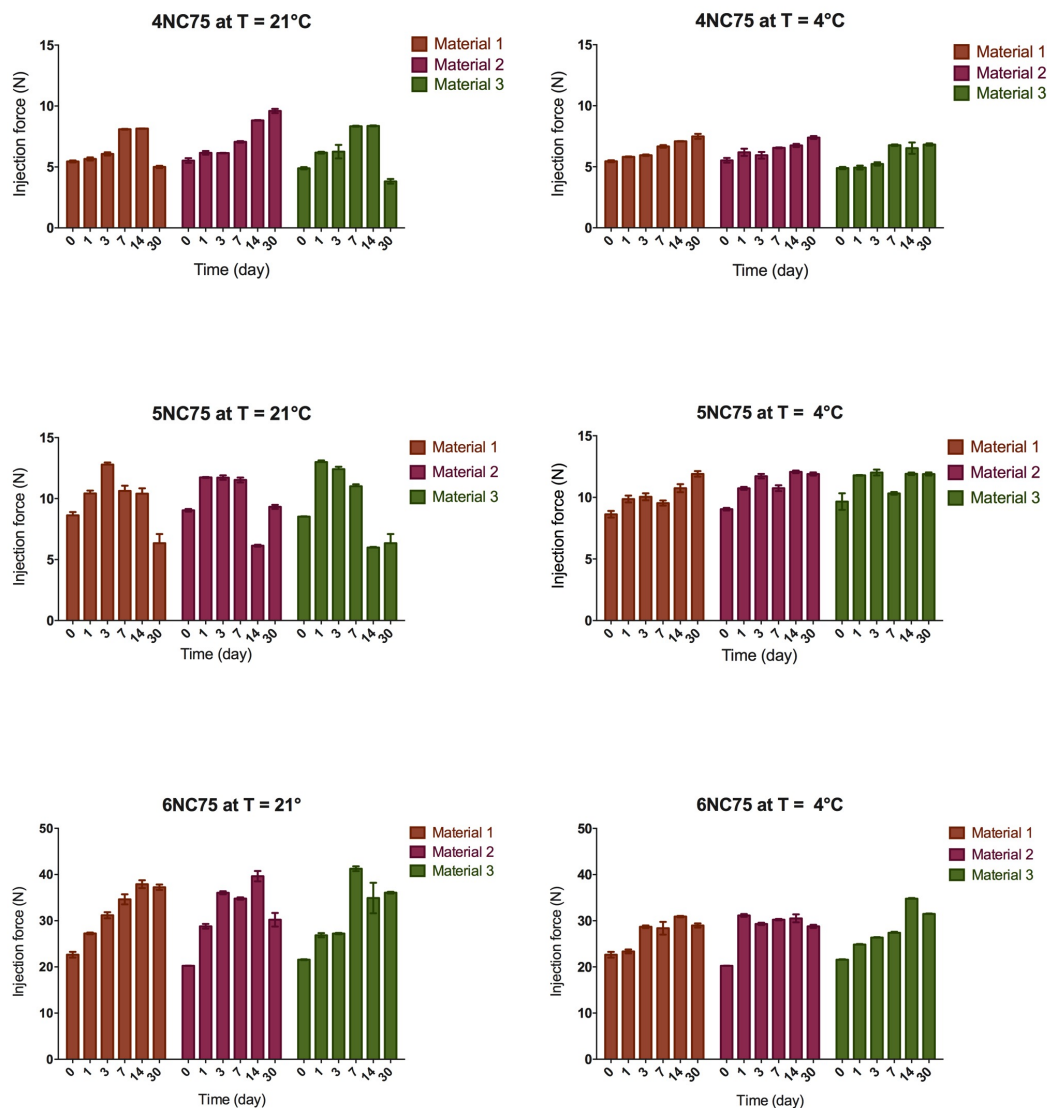


**Figure 30** – Representation of the injection force of three materials for each composition (6NC75, 5NC75, 4NC75) that were stored up to 1 month at 21°C and at 4°C. For each time point it is shown the injection force with the relative standard deviation made on three measurements.

Another experiment was performed to test the possibility to store the material in a dry state for a long period of time and then hydrate it before a further use. It was tested only on the 6NC75. It was initially studied only the possibility to freeze-dry the material and then rehydrated in order to understand if it was possible to obtain the same material after this procedure. In particular, 7.2 g of 6NC75 was frozen at -80 °C and, after 24 hours, dried to remove all the aqueous content. The solid content of the material was then vortex for 15 minutes at 3200 rpm with

6.768 ml of mill-Q water in order to hydrate it again. It would be a practical way to preserve the material in a dry state before selling and using it, having a great impact also on the costs. Unfortunately, the result was an aqueous and non-homogeneous material as is shown in the *figure 31*.

The shelf life experiments demonstrated that the best condition to store for a long period of time the developed STB in all its compositions is in a cold room at 4°C. It came to light that a low temperature could preserve the properties of the materials for a longer period of time, showing a modest increase in the injection force between 2 and 8 N.



**Figure 31-** Representation of the 6NC75 after the freeze dry process and rehydration with milli-Q water. The result is a heterogeneous and highly liquid material different from the original 6NC75.

### 3.5 Occlusion pressure

In order to evaluate the ability of the STB to withstand under the physiological pressure, it was established an in vitro model to mimic the vessel environment. The aim of the experiment was to determinate the pressure needed to remove the hydrogel from the microvasculature.

In order to simulate the microvasculature environment, the model was established using a syringe pump, connected with a syringe filled of phosphate saline buffer solution (PBS) that was inflow into a micro tube with an imposed flow rate, able to reach the systolic pressure inside of the micro tube. Four different sizes micro tubes<sup>27</sup> were tested. They were PEEK tubing with an inner diameter of 50  $\mu\text{m}$ , 100  $\mu\text{m}$ , 150  $\mu\text{m}$  and 300  $\mu\text{m}$ , and a length of 3.5 cm. The PEEK tubes were chosen, as already described in the experiment of the injectability, since they are made with one of the best material to mimic the endothelial friction coefficient. A 60 ml syringe<sup>28</sup> was filled with PBS and fixed on the syringe pump<sup>29</sup>. The syringe was then connected to a 3-way stopcock<sup>30</sup>. The other two connections of the stopcock were linked, one to the tube of the pressure sensor<sup>31</sup>, and the other one was screw with a specific PEEK adapter<sup>32</sup>. The PEEK adapter was connected, on the other side, with the micro tube. A petri dish was filled with PBS and placed in front of the syringe pump. The micro tube was insert inside of the petri dish, through a pre-made hole, so that it was completely under the PBS. The setup of the experiment is shown in the *figure 32*. Before starting the measurement, the micro

---

<sup>27</sup> PEEK tubing natural; Outer diameter: 360 $\mu\text{m}$ ; inner diameter: 25 $\mu\text{m}$ , 50 $\mu\text{m}$ , 100 $\mu\text{m}$ , 150 $\mu\text{m}$ , IDEX Health & Science.

<sup>28</sup> 60 ml BD Disposable Syringe with Luer-Lok™ Tips, Fisher scientific.

<sup>29</sup> Syringe pumps (Harvard Apparatus, PHD2000), New Era Pump Systems Inc.

<sup>30</sup> Stopcocks- 3 way with two female luer lock ports and one spin lock connector, BMG456003 B Braun medical.

<sup>31</sup> Dual pressure sensor and USB linker, Pasco.

<sup>32</sup> P-662 - FEMALE LUER TO MICROTIGHT® ASSEMBLY, F-120 - ONE-PIECE FINGERTIGHT 10-32 CONED, FOR 1/16" OD, HIDEX HEALTH & SCIENCE.



tube, connected through a PEEK adapter to a 3 ml syringe, was filled with 0.1 ml of material. The STB was tested in all the three compositions but, since the 6NC75 is not injectable in the 50  $\mu\text{m}$  tube, it was tested only with the 300  $\mu\text{m}$ , 150  $\mu\text{m}$  and 100  $\mu\text{m}$  tubes. As soon as the micro tube was filled with the material, it was immediately immersed in the PBS, because it was previously noticed that the exposure of the material to the air would affect the measurement. Once that everything was connected, the syringe pump was started using an imposed flow rate. The flow rate was previously calculated for each micro tube, in order to reach the systolic pressure of 16 kPa (120 mmHg) inside of the micro tubes filled only with the PBS. The flow rate evaluated was of 870  $\mu\text{l}/\text{min}$  for the 300  $\mu\text{m}$  tube, 320  $\mu\text{l}/\text{min}$  for the 150  $\mu\text{m}$  tube, 85  $\mu\text{l}/\text{min}$  for the 100  $\mu\text{m}$  tube and 10  $\mu\text{l}/\text{min}$  for the 50  $\mu\text{m}$  tube. The pressure was measured upstream the micro tube. When the measurement was started the pressure increased until it reached a plateau, this condition meant that the block of material started to move within the micro tube. Whereas, the sudden decreasing of the pressure showed that the material was no more occluding, and it was gone out of the micro tube. The maximum pressure reached represents the pressure that the STB can support by standing in the vessel. The pressure sensor had a maximum evaluable value of 100 kPa so, even if the needed pressure to move the material was higher than 100 kPa, it was reported 100 kPa as the maximum value.

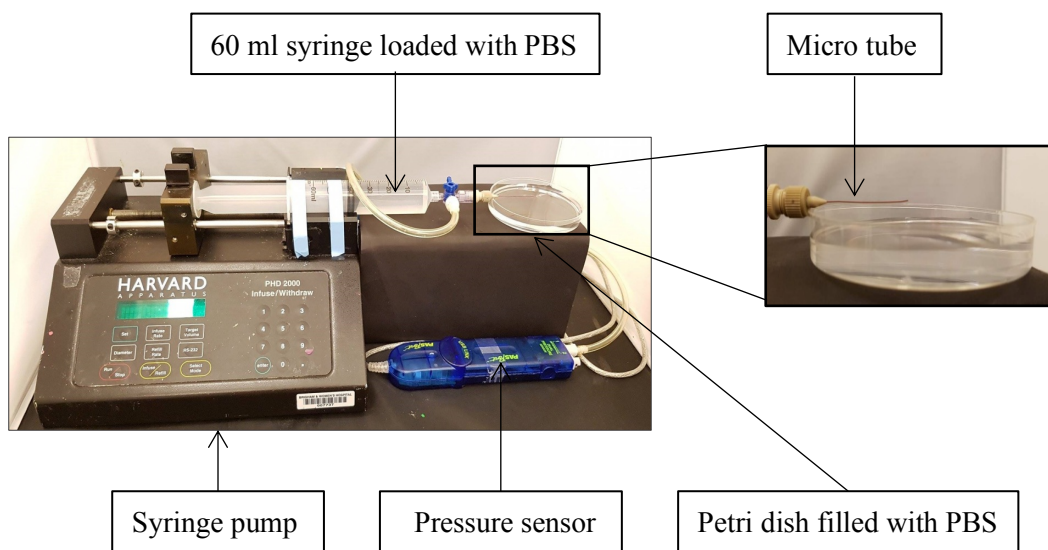


*Figure 32 - Setup of the occlusion pressure experiment.*

All the materials were tested at least three times for each micro tube and the mean of the results, with the relative standard deviations, are represented in the bar graph in the *figure 33*. It shown that the 6NC75 was able to occlude all the micro tubes. Moreover, the pressure necessary to occlude the 100  $\mu\text{m}$  tube was at least 6 times the systolic pressure, so quite impossible to reach in the blood vessels. Furthermore, the pressure needed to make the material move in the 150  $\mu\text{m}$  and the 300  $\mu\text{m}$  tubes was high enough to ensure the occlusion of the vessels. For the 5NC75 and the 4NC75, the pressure needed to remove them from the 50  $\mu\text{m}$  and 100  $\mu\text{m}$  tubes was higher than 100 kPa, so both of them would certainly occlude the smallest vasculature. Although, for the bigger tubes, with a diameter of 150  $\mu\text{m}$  and 300  $\mu\text{m}$ , the 5NC75 was occlusive, even if it could be removed under a pressure that can be reached in the normal blood vessel. Whereas, the 4NC75 was not able to occlude the 150  $\mu\text{m}$  and the 300  $\mu\text{m}$  tubes, maybe because of its softer and more liquid nature compared to the other compositions, useful to reach and occlude the smallest vessels.

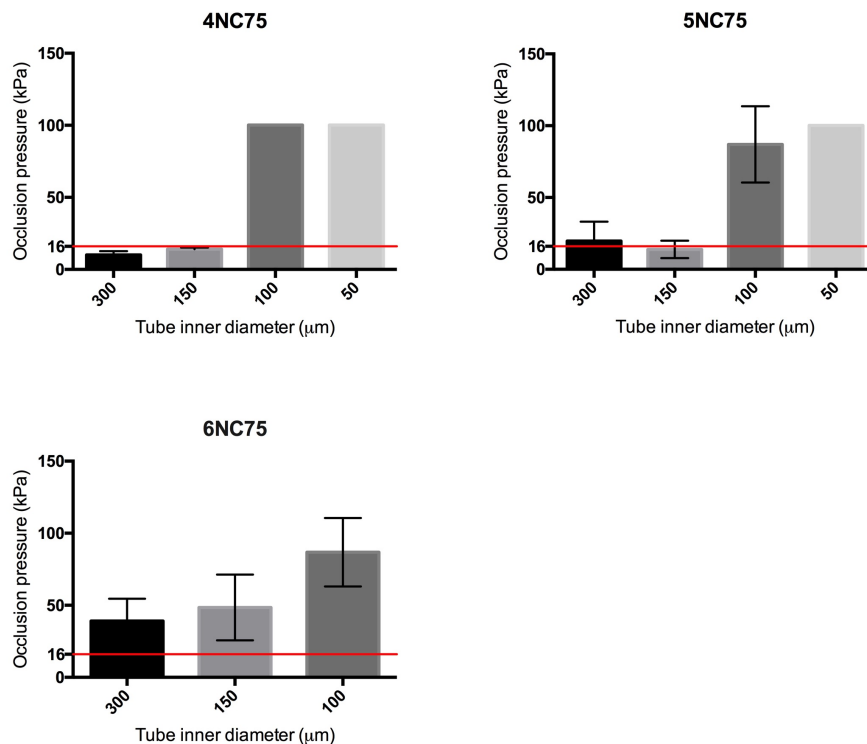


**Figure 33** - Representation of the pressure necessary to remove the 4NC75, 5NC75 and 6NC75, from different sizes micro tubes, surrounded from PBS. It is reported, for each micro tube tested and for each material, the mean of the measurements and the relative standard deviation. Moreover, it is highlighted the systolic pressure at 16 kPa.

## 4 Drug release

The functionalization of the STB with a drug would increase its therapeutic potential. The drug that was used for these experiments is the doxorubicin (DOX), since it is one of the most common chemotherapeutic drug, already used for the HCC showing great results. Loading the DOX in the STB enables the drug to affect the tumor directly from its vascularization, thus without circulating in the body and limiting its side effects. The 6NC75 was tested to be functionalized with the DOX in different ways and it was studied the correspondent drug release over time. To understand the behavior of the DOX released from the STB and their interactions, first of all it was loaded and tested the release of the DOX from only the laponite solution. In order to compare the final results, it was used a laponite gel with a concentration of 4.5% (w/v), since it is also the final concentration of laponite inside of the 6NC75. The release of the DOX was then performed from the 6NC75. It was also made a third experiment using the breakable mesoporous silica nanoparticles (MSN) to encapsulate the DOX and load the 6NC75 with them. The 6NC75 was the only composition tested as a carrier for the DOX but, since the other two STB have a lower concentration of solid particles, which means less resistance opposed to the transfer of the DOX, it can be supposed that they would have a higher release.

### 4.1 Experiment setup

All the experiments were performed evaluating the DOX released in two different media, having different pH. The phosphate buffer saline solution (PBS)<sup>33</sup>, with a pH of 7.4 and a molarity of 0.15 M, was used to simulate the physiological environment, whereas a sodium acetate buffer solution<sup>34</sup>, with pH 5.2 and a molarity of 0.15 M, was used to simulate the more acid environment characteristic

---

<sup>33</sup> Dulbecco's Phosphate-Buffered Saline (DPBS) powder (Fisher scientific) was mixed in 1L of D.I. water, (pH 7.4, 0.15M).

<sup>34</sup> Sodium acetate buffer solution (pH 5.2±0.1, 3M 0.2µm filtered), S7899-500ML, SIGMA-ALDRICH.

of the tumor. The lower pH solution was realized by diluting 1 ml of the sodium acetate buffer solution, with a molarity of 3 M, with 19 ml of milli-Q water. The solution was mixed with a vortex (with a speed of 3200 rpm) for a few seconds. In order to obtain a stock solution of DOX with a concentration of 10 mg/ml, 10 mg of DOX in powder were diluted with 1 ml of milli-Q water. The DOX is fluorescence and highly sensible to the light, so it should never be exposed to the light during the experiments. Hence, all the experiments were performed in a dark room and the samples were covered with aluminum foil.

The experiment setup for the release of the DOX from the 4.5% laponite is following described. In order to prepare a doxorubicin solution with the concentration of 1 mg/ml, 10  $\mu$ l of DOX solution were taken from the stock solution and transferred inside of a 2 ml Eppendorf. Then, 666  $\mu$ l of milli-Q water at room temperature (21°C) were added in the Eppendorf and mixed with a vortex, having a speed of 3200 rpm, for 10 seconds. Afterwards, the DOX solution was sonicated, using a water bath ultrasonic cleaner, for 30 minutes to completely disperse the DOX. The 4.5% laponite functionalized with the DOX was synthesized by putting the prepared DOX solution (with a concentration of 1mg/ml) in the ice for at least 10 minutes. This step is necessary to avoid the formation of aggregates of laponite in the final gel, slowing down the gelation and giving the time to the laponite nanoplates to completely exfoliate and organize themselves in a “house of cards” structure. The cooled down DOX solution was divided into 3 Eppendorf of 2 ml. In this way, in each Eppendorf there were 222  $\mu$ l of milli-Q water and 3.3333  $\mu$ l of DOX solution. The final hydrogel was obtained by adding 0.01 g of laponite powder to each Eppendorf and mixing them with a vortex (with a speed of 3200 rpm) for at least 10 minutes. The resulting functionalized 4.5% laponite is shown in the *figure 34*. It had a concentration of DOX of 0.148 mg/ml and an initial mass of DOX dispersed inside each sample of 33.33  $\mu$ g. It was still transparent and presented a red coloration given by the DOX.

The 3 Eppendorf were then centrifuged with a mini centrifuge<sup>35</sup> for 10 seconds and beaten against a desk in order to have a flat surface. On the top of each sample were added 250 µl of PBS, with a pH of 7.4 and a molarity of 1.5 M, after that the samples were stored at 37 °C, in order to simulate the physiological environment. At each time-point all the PBS was taken off from the samples and 200 µl of it were collected in a black 96 well plate<sup>36</sup>. The PBS was replaced with 250 µl of a new one and stored again at 37 °C until the next time point. The time points were fixed at 1,2,4,8,24 hours, 3,7,14,30 days. The fluorescence of the collected samples was immediately measured with the micro plate reader<sup>37</sup> setting an excitation of 485 nm and an emission of 590 nm.



**Figure 34** - Representation of the 4.5% laponite functionalized with the doxorubicin, having a concentration of 0.148 mg/ml.

---

<sup>35</sup> Mini Centrifuge, power 115-240 Volt 50/60 Hz, Max. speed/force: 6600rpm/2200xG, Capacity: 0.2 ml, Fisher Scientific (05-090-100).

<sup>36</sup> Corning® 96 Well Black Polystyrene Microplate, (clear flat bottom, black polystyrene plate (Ideal for fluorescent assays), matrix active group TC-treated, pkg of (individually wrapped), sterile, lid), SIGMA-ALDRICH®.

<sup>37</sup> Luminescence microplate reader (absorbance / fluorescence / multi-mode), 6 - 1 536 well, Synergy 2, BioTek®.

At the same time the DOX release experiment was performed from the 6NC75. The realization of the samples started with the normal preparation of the 6NC75, which was performed as described in the chapter 2. After the last step of the preparation of the 6NC75, which consist in leaving the material in the water bath at 45 °C for 10 minutes, 0.72 g of the STB were transferred in a 2 ml Eppendorf. The DOX was transferred from the stock solution to the Eppendorf in the amount of 10.18 µl and the solution was immediately mixed. The temperature of the 6NC75, that was still warm from the water bath when was mixed with the DOX, could help the dispersion of the DOX. The solution was mixed with a vortex using a speed of 3200 rpm for 15 minutes. Moreover, each 5 minutes the vortex was stopped and the material was mixed by hand using a spatula in order to homogenized more the DOX within it. Afterwards, the material was centrifuged with a mini centrifuge and beaten against a desk in order to obtain a flat surface. Before starting the drug release experiment, the material was stored at room temperature (21°C) for 1 hour, to ensure the establishment of the bonds inside of the material itself. The amount of DOX was chosen to obtain the same concentration of DOX present in the previous tested sample with the 4.5% laponite. Thus, the final concentration of DOX in the 6NC75 was of 0.148 mg/ml with an initial mass of 101,8 µg of DOX.

Three samples of the functionalized 6NC75 were prepared in the described way and, after 1 hour of rest, 250 µl of PBS were added to each sample that were then stored at 37°C. After each time point, that was fixed as for the previous experiment (1,2,4,8,24 hours, 3,7,14,30 days), 200 µl of the supernatant were collected in a 96 black well plate and evaluated with the micro plate reader, using an excitation of 485 nm and an emission of 590 nm. The PBS was replaced with 250 µl of a new one and the samples were stored at 37°C until the next time point. It was not possible to test the injection force of the functionalized STB, due to the small amount of material that could be produced. However, for what concern the elasticity and density that could be tested by touching the material, it looked like the 6NC75 without the DOX. The visual aspect, that is represented in the *figure 35*, showed a red coloration, given from the presence of the DOX. Moreover, compared

with the laponite-DOX sample, it was not transparent and presented a more intense coloration.



*Figure 35 - Representation of the 6NC75 functionalized with the doxorubicin having a concentration of 0.148 mg/ml.*

The last experiment that was performed, regarding the functionalization of the STB with the DOX, was made using also the mesoporous silica nanoparticles (MSN). The MSN are spherical nanoparticles, breakable under reducing conditions, with a size of 100 nm in diameter and a pore diameter of 2.3 nm, easily penetrable by the doxorubicin particles. The Z-potential in PBS (pH 7.4) is known to be of  $-13.3 \pm 1.3$  mV, therefore the MSN can electrostatically interact with the positive charge of the doxorubicin. The MSN were used to have a more controlled release ratio of the DOX and at the same time make the release more selective to the tumor, since the MSN would break down when surrounded from a reducing media such as the one present in the tumor environment. Thus, the DOX can be easily encapsulated by the MSN and then released when goes inside of the tumor. The preparation of the STB functionalized with the MSN and the DOX, started with the normal preparation of the 6NC75 as it is described in the chapter 2. The MSN stock solution was prepared by dispersing 10 mg of MSN powder in 10 ml of milli-Q water. The solution was sonicated for 30 minutes, using a water bath ultrasonic cleaner, and then incubated for 1 hour at 45°C in the water bath. This procedure

was repeated for 3 times in order to obtain a homogeneous solution of milli-Q water and MSN with a concentration of 1 mg/ml of MSN. The functionalization of the MSN with the DOX is obtained by adding 10.18  $\mu$ l of DOX from the stock solution (with a concentration of 10 mg/ml) to 10.18  $\mu$ l of MSN stock solution and vigorously mixing them for 10 minutes, using a vortex with a speed of 3200 rpm. The 6NC75 is taken after the 10 minutes of incubation at 45°C and mixed with the MSN-DOX solution in a 2 ml Eppendorf using the following ratio, 0.72 g of STB and 20.32  $\mu$ l of the MSN-DOX solution. It was mixed with a vortex (having a speed of 3200 rpm) for 15 minutes and, to obtain a homogeneous gel, each 5 minutes it was mixed by hand with a spatula for a few seconds. The Eppendorf was then centrifuged for 10 seconds with the mini-centrifuge and beaten against the desk in order to have a flat surface. The final material was stored for 1 hour before any further use. As shown in the *figure 36*, the visual appearance was similar to the STB with only the DOX, it had a red color given by the DOX, which in its original powder is brightly red. The final concentration of DOX was of 0.146 mg/ml, so almost the same concentration used in the previous two experiments. The initial mass of DOX dispersed in each sample was of 101.8  $\mu$ g. Whereas, the final concentration of the MSN in the sample was of 0.0146 mg/ml.

The release experiment was started with the same procedure used for the previous experiments. Three sample were prepared as above described and covered with 250  $\mu$ l of PBS. The samples were then incubated at 37° C until each time point. The time point was fixed at 1,2,4,8,24 hour and 3,7,14,30 days. After each time point, 200  $\mu$ l of the supernatant were collected in the 96 black well plate and all the PBS was substituted with 250  $\mu$ l of a new one. The measurements of the fluorescence were made with the micro plate reader (excitation of 485 nm and emission of 590 nm).

The mass of DOX released from each sample, for all the performed experiments, was evaluated reading the fluorescence of the DOX. It was possible to read the fluorescence of the DOX using a luminescent micro plate reader by setting the excitation at 485 nm and the emission at 590 nm. The chosen wave lengths were already tested in the laboratory as the best one in order to detect the presence of DOX.





*Figure 36 - Representation of the 6NC75 functionalized with the mesoporous silica nanoparticles and the doxorubicin, having a final concentration of DOX of 0.146 mg/ml.*

The three experiments were all repeated with the same procedure but using the sodium acetate buffer solution instead of the PBS. The sodium acetate buffer solution had the same molarity of the PBS but a pH 5.2. The experiments were repeated using a lower pH since it should be more representative of the acid conditions inside of the tumor. Moreover, the DOX (doxorubicin hydrochloride) present a different hydrophilicity under different pH conditions. When it is under acid condition it maintain its salt form that is soluble in water. Whereas, when the pH is set at 7.4 the DOX is able to dissociate into neutral hydrophobic molecule. Thus, the release from a medium with a pH 5.2 should be higher than in physiological condition (pH 7.4). Furthermore, from previous studies it has been demonstrated that the DOX released from the laponite should increase when the pH is decreased. It has been also demonstrated that, under higher pH, the laponite-DOX conformation change forming larger aggregation that may limit the release of DOX due to the extended diffusion distance that the DOX should do. For the same reason, also the DOX released from the 6NC75 and the 6NC75 functionalized with the MSN should be faster under a lower pH [24].

## 4.2 Results

The DOX release in the media was evaluated by its fluorescence, using a micro plate reader. In order to calculate the mass of DOX released from the sample, correspondent to the read fluorescence, the following calibration curve was evaluated (*figure 37*). The calibration curve was realized by making 18 different concentrations of DOX between 0.0002 mg/ml and 0.003 mg/ml. The range of concentrations evaluated was correspondent to the range of DOX released from the samples. The different concentrations were realized by diluting the initial DOX stock solution with the required amount of milli-Q water. For each concentration, 200 µl of the solution were transferred in a 96 black well plate. The well plate was then measured using a micro plate reader, setting the wave length of the excitation at 485 nm and the one of the emission at 590 nm.

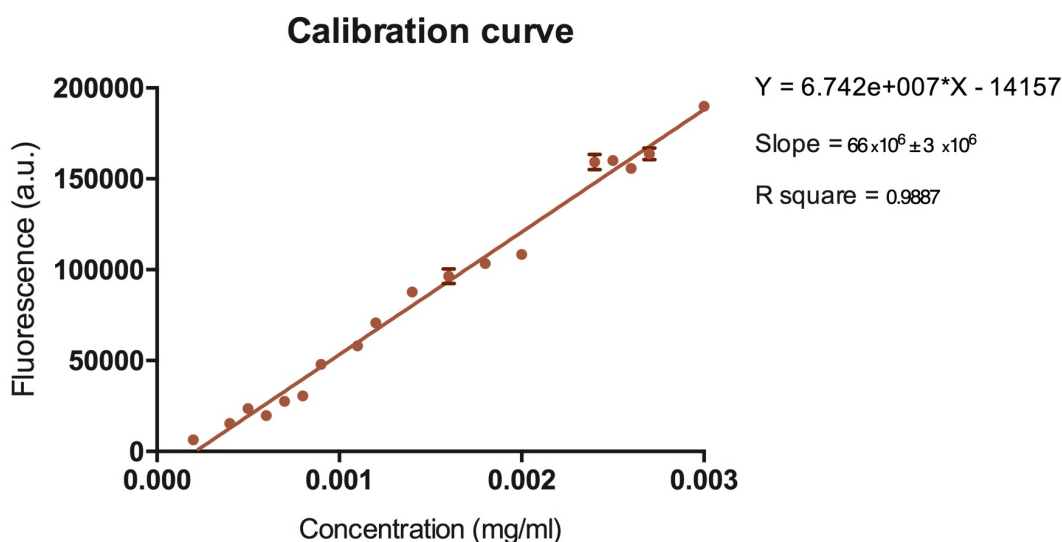


**Figure 37** – Representation of the calibration curve realized using different concentrations of doxorubicin (between 0.0002 and 0.003) read with the luminescent micro plate reader using an excitation of 485 nm and an emission of 590 nm.

The mass of DOX released in the measured samples was then calculated using the equation of the calibration curve as shown in the following equations.

$$y = 6.721 \times 10^7 x - 14157 \quad (5)$$

$$c = \frac{(f + 14157)}{6.742 \times 10^7} \quad (6)$$

$$m = c \times v \quad (7)$$

$$\% \text{ DOX released} = \frac{m}{m_i} \times 100 \quad (8)$$

The equation (5) represents the calibration curve, from which it is possible to calculate the concentration of DOX ( $x$ ) correspondent to the read fluorescence ( $y$ ). The concentration, that is evaluated through the equation (6), is indicated with  $c$ , whereas the fluorescence is represented by  $f$ . The total mass of the DOX released ( $m$ ) is evaluated by the equation (7) multiplying the concentration ( $c$ ) by the total volume of the medium ( $v$ ), that for example in the samples in the experiments described correspond to 250  $\mu\text{l}$ . The percentage of total DOX released from the sample and normalized by the initial mass of DOX, is evaluated by the equation (8). Here the  $m_i$  is the initial mass of DOX dispersed inside the sample before starting the release experiment. Each experiment was performed using three samples, and each measurement of the fluorescence was repeated three times. The final percentage of mass released was evaluated as the mean of the three measurements of the single sample and represented by the mean of the three samples with the relative standard deviation for each experiment performed. The final results are represented in the *figure 38, 39 and 40*, which report the cumulative DOX release, in different pH medium, respectively from the 4.5% laponite, the 6NC75 and the 6NC75 with the MSN. Comparing the results of the different materials used, it emerges that by increasing the mass of the samples, which can oppose resistance to the transfer of the DOX, the release rate tends to decrease. Thus, the DOX release is higher in the laponite and tends to decrease in the STB

and STB with MSN, where the interactions between the laponite and the gelatin generate a more complex structure inside of the material that can oppose resistance to diffusion of the DOX. Analyzing the single material in the different pH conditions, it can be observed that the 6NC75 with the MSN (*figure 38*) present a higher release correspondent to the lower pH, in accord with what was expected, and during the first hours no burst release can be observed. Whereas, the release from the STB (*figure 39*) and from the 4.5% laponite (*figure 40*) represent an opposite trend, showing a faster release associated with a higher pH, in conflict with what can be deduced from the theory. These results may be attributed to the inappropriate setup of the experiment performed inside the Eppendorf, since the diffusion of the DOX in the outside solvent is restricted to the only upper surface, whereas the rest of the material is kept intact by the surrounding tube wall. Therefore, the low pH does not show the expected outcome due to the less impact on the material from the surrounding medium. Thus, the experiments setup was modified in order to overcome this problem and perform the experiment in a more appropriate way.

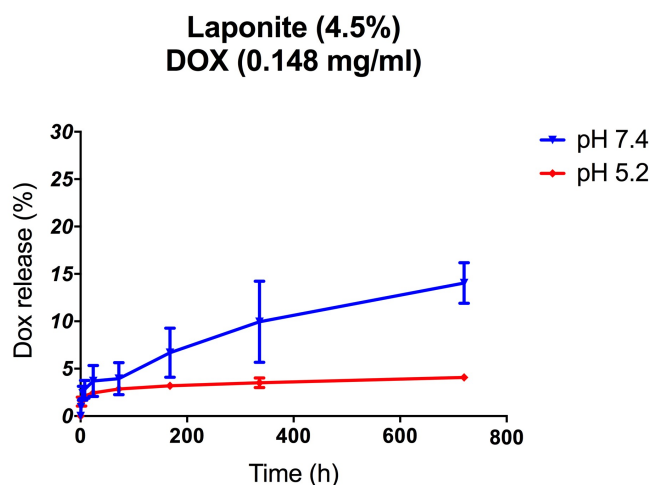


**Figure 38** - Representation of the percentage of the cumulative doxorubicin released from the 4.5% laponite, with a concentration of DOX of 0.148 mg/ml, in two different media having the pH 7.4 and pH 5.2. It is represented the mean of the three different samples, for each one of which of the fluorescence was measured three times, and the relative standard deviation.

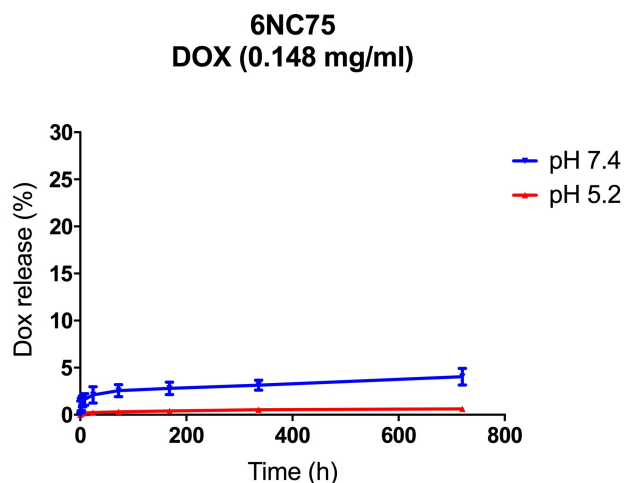


**Figure 39** - Representation of the percentage of the cumulative doxorubicin released from the 6NC75, with a concentration of DOX of 0.148 mg/ml, in two different media having the pH7.4 and pH5.2. It is represented the mean of the three different samples, for each one of which of the fluorescence was measured three times, and the relative standard deviation.

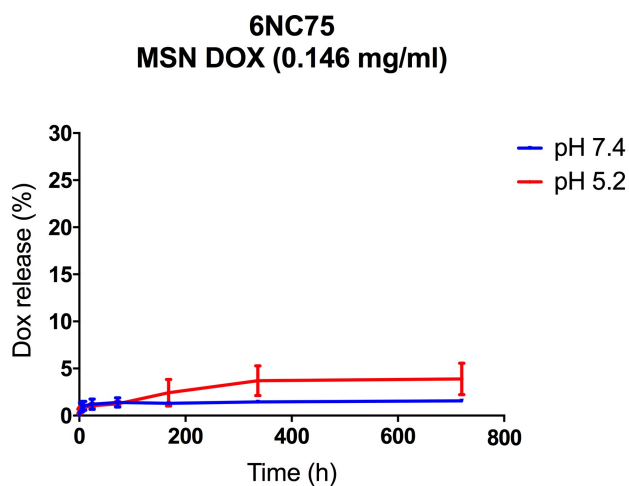


**Figure 40** - Representation of the percentage of the cumulative doxorubicin released from the 6NC75 with mesoporous silica nanoparticles and having a concentration of DOX of 0.146 mg/ml, in two different media having the pH7.4 and pH5.2. It is represented the mean of the three different samples, for each one of which of the fluorescence was measured three times, and the relative standard deviation.

### 4.3 Experiment optimization

The experiments of the drug release, from the different tested materials, were repeated changing the experiments setup. In order to ensure a bigger surface of the material in contact with the medium, the experiments were performed using a 24 well plate<sup>38</sup> instead of the Eppendorf. The three different materials, 4.5% Laponite, 6NC75 and 6NC75 with MSN, were realized and functionalized using the same ratio and concentration of DOX of the previous experiments. The study of the release was then performed using the following procedure.

For each composition, 0.1 ml of material were transferred, through the use of a 3 ml syringe with a 32 G needle, inside of a 24 well plate and covered with 600 µl of PBS (pH 7.4, 1.5 M) or of sodium acetate buffer solution (pH 5.2, 1.5M). The samples were injected in the well of the plate trying to obtain the same shape in all of them. The first line of the well plate was filled with six samples of laponite, the second with six samples of STB, whereas the third line was filled with six samples of STB with MSN. The first three column of the well plate were covered with the PBS, whereas the other three were covered whit the sodium acetate buffer solution. The final 24 well plate is represented in the *figure 41*. The so composed 24 well plate was stored at 37 °C and, at each time point (that were set as for the previous experiments at 1,2,4,8,24 hours and 3,7,14,30 days), 200 µl of supernatant were collected in a black 96 black well plate and read with a micro plate reader, setting the excitation at 485 nm and the emission at 590 nm. The medium was completely removed from the samples and replaced with 600 µl of a new one. The concentration of DOX in each sample was the same of the previous experiment, whereas the initial mass of DOX was of 0.014 mg for all the materials.

---

<sup>38</sup> Falcon™ Tissue Culture Plates, 24-well; Standard tissue culture; Flat-bottom; Growth area: 2cm<sup>2</sup>; Well volume: 3.5mL; 1/Tray, Fisher Scientific.

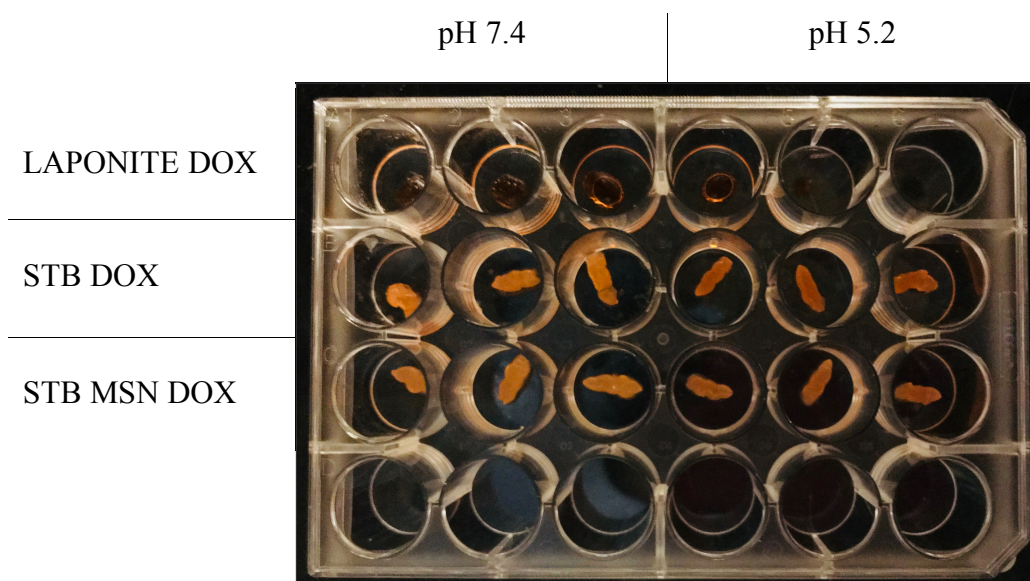


**Figure 41** - 24 well plate filled with the samples of 4.5% laponite, 6NC75 and 6NC75 with MSN, functionalized with the doxorubicin.

The results, that are reported in the *figure 42,43 and 44*, show a faster release of the DOX, from all the three materials tested, compared to the results of the experiments performed in the Eppendorf. These results could be expected, because now the materials are all surrounded by the medium and in this way the diffusion in the solvent is facilitated. Analyzing the single materials, it can be noticed that the release of the DOX from the 4.5% laponite is still lower when the pH is 5.2, even if after the first week the release seems to start to get higher. This result is not in agreement with the theory, so the experiment need to be repeated since it is unreliable (*figure 42*). It was probably due to an observable faster degradation of the sample when it was dispersed in the PBS. Regarding the 6NC75 and the 6NC75 functionalized with the MSN, that are respectively represented in the *figure 43 and 44*, it is possible to see how the release of DOX is really higher at a lower pH (pH 5.2) than at pH 7.4. These results represent a promising potential for the chemotherapeutic behavior of the STB, since the pH of the tumor site is generally between 5 and 6 so the release of DOX, when the material would reach the target tumor, would be consistent.

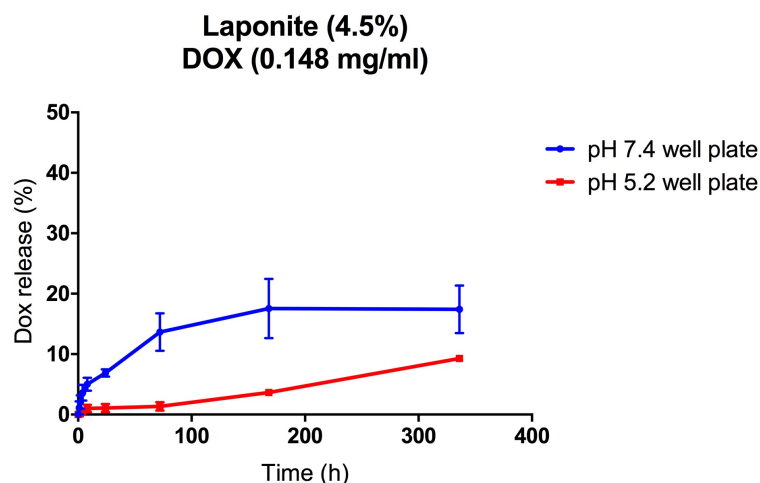


**Figure 42** - Representation, for the experiment performed in the well plate, of the percentage of the cumulative doxorubicin released from the 4.5% laponite, with a concentration of DOX of 0.148 mg/ml, in two different media having the pH 7.4 and pH 5.2. It is represented the mean of the three different samples, for each one of which of the fluorescence was measured three times, and the relative standard deviation.

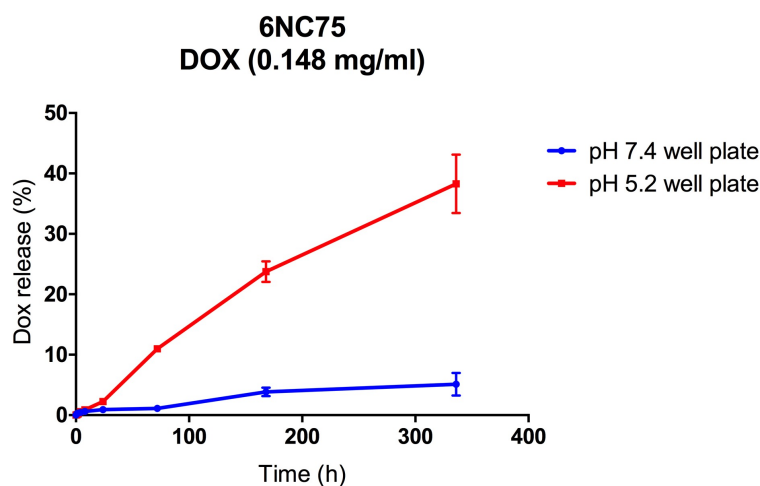


**Figure 43** - Representation, for the experiment performed in the well plate, of the percentage of the cumulative doxorubicin released from the 6NC75 with a concentration of DOX of 0.148 mg/ml in two different media having the pH 7.4 and pH 5.2. It is represented the mean of the three different samples, for each one of which of the fluorescence was measured three times, and the relative standard deviation.



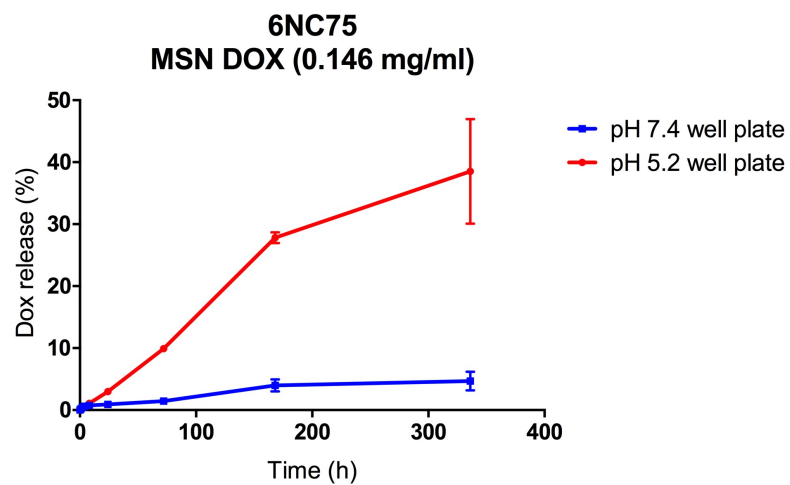


**Figure 44** - Representation, for the experiment performed in the well plate, of the percentage of the cumulative doxorubicin released from 6NC75-MSN with a concentration of DOX of 0.146 mg/ml in two different media having the pH 7.4 and pH 5.2. It is represented the mean of the three different samples, for each one of which of the fluorescence was measured three times, and the relative standard deviation.

## 5 Conclusions

The aim of this project was to realize and analyze a new shear-thinning biomaterial for chemoembolization. It was developed with a particular interest for a future application in the treatment of the hepatocellular carcinoma, the main tumor of the liver. The distinctive shear-thinning behavior of the material, enables it to be easily injectable in the smallest vasculature of the tumor and at the same time to stand in the reached position under a relative high pressure. This singular characteristic is obtained by the use of the laponite and its interaction with the gelatin. There were realized three materials having different ratio of laponite and gelatin, labelled as 4NC75, 5NC75 and 6NC75 respectively. It was noticed that, by increasing the amount of solid particles, the material became more viscous. Depending on the composition, and on its viscosity, the material could be used to occlude different portions of the tumor vasculature, according to their size. All of the three compositions were characterized by some in vitro experiments to understand their behavior in the physiological environment. The experiments showed that all the three materials were easily injectable in micro tubes having an inner diameter between 100  $\mu\text{m}$  and 300  $\mu\text{m}$ , which are comparable to the inner diameter of the capillaries of the tumor. Furthermore, the materials proved a great stability under simulated physiological conditions, without showing any degradation or swelling behavior when incubated, up to 1 month at 37 °C, surrounded by PBS. Moreover, the shelf life of the material, in all its compositions, was evaluated. It was found out that, the best way to preserve the properties of the materials for a long term, is their storage at low temperature as 4 °C. It was also demonstrated that they can withstand, in a simulated microvasculature environment, without being removed when subjected to a pressure higher than the systolic one. Finally, the 6NC75 was functionalized using one of the most commonly used chemotherapeutic drug, the doxorubicin (DOX). The release of the DOX over time was evaluated using two different media, one with a pH 7.4, to represent the physiological environment, and the other one with a pH 5.2 in order to simulate the tumor environment. Moreover, in order to obtain a more controlled and selective release of the DOX, the 6NC75 was functionalized with the

mesoporous silica nanoparticles (MSN), which are able to embody the DOX and break down their structure, releasing their content, under a reducing agent. The experiments were performed using two different setups. Initially they were executed using the Eppendorf as a holder for the material, afterwards, in order to have a bigger surface of the material in contact with the medium, so that the diffusion in the solvent was facilitated, it was performed using a 24 well plate. The results showed that, by increasing the amount of solid content, which could hinder the transfer of DOX, the release was slower. Furthermore, in the experiments performed in the well plate, the release was greater when the materials were in contact with a medium having a lower pH. The highest results were obtained using the 6NC75 and the 6NC75 functionalized with the MSN, in an acid environment and using the well plate as a container. That demonstrates the high potential of the functionalization of the 6NC75 with the DOX, in order to achieve a high selective chemotherapy of the tumor. Further study should be done to investigate the potential breakdown ability of the MSN in a reducing environment, as it could consistently increase the release of the DOX into the tumor. Moreover, the drug release experiments should also be performed on the 4NC75 and 5NC75 in order to fully characterized them. In conclusion, during the analysis carried out, it became apparent that the realized STB, in all the tested compositions, presents great qualities that would allow it to be used for chemoembolization. Furthermore, depending on the composition, the materials can be used for the occlusion of different sizes vessels.

## **5.1 Future directions**

To translate the knowledge acquired on these new shear-thinning biomaterials in a clinical application, further studies are needed. The analysis of the cytotoxicity of the DOX is necessary to understand the initial concentration of DOX required in the STB, in order to obtain an efficient treatment of the tumor. Furthermore, some *ex vivo* experiments should be performed to better understand the injectability of the material, its penetration depth and the degree of occlusion. These experiments could consist in the injection of the materials in a decellularized liver of a rat and in the subsequent analysis by micro-CT and histology, in order to understand both their injectability and penetration depth. Finally, some *in vivo* experiments would be the last step to characterize the materials and see their real efficiency in the treatment of the hepatocellular carcinoma.

The developed shear-thinning biomaterials have shown good properties for a new minimally invasive biomedical procedure, which may shape the future of current practice in cancer research.

## List of Figures

<b>Figure 1</b> - Angiogenesis of the tumor. A) Tumor at the first stadium, without vascularization; B) Hypoxia induce the production of angiogenic factors that stimulate the angiogenesis; C) Vascularized tumor. (Source: <a href="http://www.mdpi.com/1422-0067/18/9/1967/htm">http://www.mdpi.com/1422-0067/18/9/1967/htm</a> ) .....	2
<b>Figure 2</b> - Comparison between a normal organized vascularization and the abnormal vascularization of the tumor. (Source: <a href="http://memorize.com/ebme-unit-1-cancer-case-study/ndifranco94">http://memorize.com/ebme-unit-1-cancer-case-study/ndifranco94</a> ).....	2
<b>Figure 3</b> - Chemoembolization of the liver carcinoma procedure.....	7
<b>Figure 4</b> - Schematic representation of the gelation of the laponite. It shows the chemical structure of a single disk of laponite and the single steps from the dry state to the “house of cards” structure of the laponite when is dispersed in water. (Source: BYK, technical information B-RI 21, LAPONITE-Performance Additives) .....	10
<b>Figure 5</b> - Schematic representation of the shear-thinning hydrogel from the mix of gelatin with laponite. ....	11
<b>Figure 6</b> - Functionalization of the laponite and the final STB with the doxorubicin (DOX). ....	12
<b>Figure 7</b> - Functionalization of the MSN with the DOX and break down of the MSN particles when are in contact with the tumor cell.....	13
<b>Figure 8</b> - Final Laponite transparent gel.....	15
<b>Figure 9</b> - Final 6NC75, whit in color and sticky to the wall of the falcon tube..	16
<b>Figure 10</b> - Position of the material on the vortex.....	17
<b>Figure 11</b> - Setup of the Instron to measure the injection force of the material...	19
<b>Figure 12</b> - On the left it is represented the injection force of a homogeneous material, whereas on the right it is represented the injection force of a non-homogeneous one. ....	19

<b>Figure 13</b> - There are represented the bar graphs of the injection force of the 6NC75, the 5NC75 and the 4NC75 with the respective standard deviations. It is possible to observe the value of the injection force and to notice the reproducibility of all the three compositions. ....	20
<b>Figure 14</b> - Representation of the injection force of seven materials tested using a warm milli-Q in the protocol for the 6NC75. In all the graphs it is observable a flat plateau, characteristic of a homogeneous material.....	22
<b>Figure 15</b> - Bar graph to compare the values of the injection forces of the different materials tested using the warm milli-Q water in the protocol. It can be seen that the values of the injection forces are highly different between the tested materials, highlighting the non-reproducibility of this method.....	22
<b>Figure 16</b> - <i>6NC75 made with warm milli-Q water. It is possible to see a more transparent aspect compared to the material produced with the standard protocol and showed in the figure 9.</i> ....	23
<b>Figure 17</b> – Representation of the injection forces of the three materials tested using a cold water in the protocol of the 6NC75. In the graphs of the material 2 and 3, it is clearly visible the presence of bumps, which represent the non-homogeneity of the materials. ....	24
<b>Figure 18</b> – Representation in a bar graph of the injection forces of the three materials tested using the cold water in the protocol of the 6NC75. It can be observed that the values of the injection forces are highly different between the tested materials, highlighting the non-reproducibility of this method.....	24
<b>Figure 19</b> - Representation of the injection forces of the 6NC75 realized with 3 hours of mixing at room temperature. For each material the measurement was repeated three times. It is clearly visible the non-homogeneity of the materials.....	26
<b>Figure 20</b> – There are compared, in a bar graph, the injection forces of the three materials made with 3 hours of mixing at room temperature. It is observable the non-reproducibility of the material using this method. ....	26

<b>Figure 21-</b> Representation of the injection force of the 6NC75 realized with a mixing time of 3 hours performed in the cold room (4°C). Each measurement was repeated three times to be consistent. The results show numerous bumps in the graph, synonymous of the non-homogeneity of the materials. ....	27
<b>Figure 22 –</b> Bar graph of the injection forces of the 6NC75 realized with 3 hours of mix in the cold room (4 °C). It shows a difference between the injection forces of the three materials tested, representing a non-reproducibility of the 6NC75 using this method.....	28
<b>Figure 23 -</b> A comparison between the 6NC75 realized with 3 hours of mixing time at 21°C (I), 3 hours of mixing time at 4°C (II) and the material realized using the standard protocol (III). ....	28
<b>Figure 24 -</b> Comparison between the injected 6NC75 realized with 3 hours of mixing at 21°C (I), 3 hours of mixing at 4°C (II) and with the standard protocol (III). It is visible how the material I and II spread out when injected, whereas the III is able to form a standing structure.....	29
<b>Figure 25 -</b> Summary of the injectability of the materials through micro tubes with different inner diameter.....	31
<b>Figure 26 -</b> Comparison between the three different compositions of the material injected through micro tubes with an inner diameter of 100 µm. ....	31
<b>Figure 27 -</b> Representation, for the 4NC7,5 5NC75 and 6NC75, of the percentage of solid content of the samples, up to one month after their incubation at 37°C in contact with PBS. For each time point it is reported the mean of the values of the solid content of three samples, with the respective standard deviation.....	34
<b>Figure 28 -</b> Representation of the percentage of swelling for the 4NC75,5NC75 and 6NC75 when are incubated up to 1 month at 37°C surrounded with PBS. ....	37
<b>Figure 29 -</b> It is shown the 4NC75 store for 24 hours at - 20°C. It is possible to see a completely phase separation between the liquid and the solid components of the material. ....	39
<b>Figure 30 –</b> Representation of the injection force of three materials for each composition (6NC75, 5NC75, 4NC75) that were stored up to 1 month at 21°C and	

at 4°C. For each time point it is shown the injection force with the relative standard deviation made on three measurements. ....	41
<b>Figure 31-</b> Representation of the 6NC75 after the freeze dry process and rehydration with milli-Q water. The result is a heterogeneous and highly liquid material different from the original 6NC75. ....	42
<b>Figure 32 -</b> Setup of the occlusion pressure experiment. ....	44
<b>Figure 33 -</b> Representation of the pressure necessary to remove the 4NC75, 5NC75 and 6NC75, from different sizes micro tubes, surrounded from PBS. It is reported, for each micro tube tested and for each material, the mean of the measurements and the relative standard deviation. Moreover, it is highlighted the systolic pressure at 16 kPa. ....	45
<b>Figure 34 -</b> Representation of the 4.5% laponite functionalized with the doxorubicin, having a concentration of 0.148 mg/ml. ....	48
<b>Figure 35 -</b> Representation of the 6NC75 functionalized with the doxorubicin having a concentration of 0.148 mg/ml. ....	50
<b>Figure 36 -</b> Representation of the 6NC75 functionalized with the mesoporous silica nanoparticles and the doxorubicin, having a final concentration of DOX of 0.146 mg/ml. ....	52
<b>Figure 37 –</b> Representation of the calibration curve realized using different concentrations of doxorubicin (between 0.0002 and 0.003) read with the luminescent micro plate reader using an excitation of 485 nm and an emission of 590 nm. ....	53
<b>Figure 38 -</b> Representation of the percentage of the cumulative doxorubicin released from the 4.5% laponite, with a concentration of DOX of 0.148 mg/ml, in two different media having the pH 7.4 and pH 5.2. It is represented the mean of the three different samples, for each one of which of the fluorescence was measured three times, and the relative standard deviation. ....	55
<b>Figure 39 -</b> Representation of the percentage of the cumulative doxorubicin released from the 6NC75, with a concentration of DOX of 0.148 mg/ml, in two different media having the pH7.4 and pH5.2. It is represented the mean of the three	



different samples, for each one of which of the fluorescence was measured three times, and the relative standard deviation..... 56

**Figure 40** - Representation of the percentage of the cumulative doxorubicin released from the 6NC75 with mesoporous silica nanoparticles and having a concentration of DOX of 0.146 mg/ml, in two different media having the pH7.4 and pH5.2. It is represented the mean of the three different samples, for each one of which of the fluorescence was measured three times, and the relative standard deviation..... 56

**Figure 41** - 24 well plate filled with the samples of 4.5% laponite, 6NC75 and 6NC75 with MSN, functionalized with the doxorubicin..... 58

**Figure 42** - Representation, for the experiment performed in the well plate, of the percentage of the cumulative doxorubicin released from the 4.5% laponite, with a concentration of DOX of 0.148 mg/ml, in two different media having the pH 7.4 and pH 5.2. It is represented the mean of the three different samples, for each one of which of the fluorescence was measured three times, and the relative standard deviation..... 59

**Figure 43** - Representation, for the experiment performed in the well plate, of the percentage of the cumulative doxorubicin released from the 6NC75 with a concentration of DOX of 0.148 mg/ml in two different media having the pH 7.4 and pH 5.2. It is represented the mean of the three different samples, for each one of which of the fluorescence was measured three times, and the relative standard deviation..... 59

**Figure 44** - Representation, for the experiment performed in the well plate, of the percentage of the cumulative doxorubicin released from 6NC75-MSN with a concentration of DOX of 0.146 mg/ml in two different media having the pH 7.4 and pH 5.2. It is represented the mean of the three different samples, for each one of which of the fluorescence was measured three times, and the relative standard deviation..... 60

## Bibliography

- [1] L. R. Roberts and J. D. Yang, "Hepatocellular carcinoma: a global view," *Nature*, vol. 7, August 2010.
- [2] M. Sangiovanni and A. Colombo, "Treatment of hepatocellular carcinoma: beyond international guidelines," *Liver International*, 2015.
- [3] A. Forner, J. M. Llovet and J. Bruix, "Hepatocellular carcinoma," *Seminar*, 2012.
- [4] A. Di Leo and G. M. Saracco, "Tumori epatici," in *Manuale di gastroenterologia UNIGASTRO*, Editrice Gastroenterologica Italiana S.r.l., 2013-2015.
- [5] N. Nishida, H. Yano, T. Nishida, T. Kamura and M. Kojiro, "Angiogenesis in cancer," *Vascular Health and Risk Management*, 2006.
- [6] M. Fernandez, D. Semela, J. Bruix, I. Colle, M. Pinzani and J. Bosch, "Angiogenesis in liver disease," *Journal of Hepatology*, 2009.
- [7] J. M. Berg, J. L. Tymoczko and L. Stryer, "Cancro e glicolisi," in *BIOCHIMICA quinta edizione*, Zanichelli.
- [8] Y.-X. J. Wáng, T. De Baere, J.-M. Idée and S. Ballet, "Transcatheter embolization therapy in liver cancer: an update of clinical evidences," *Chinese Journal of Cancer Research*, vol. 27, no. 2, April 2015.
- [9] B. VOLLMAR and M. D. MENDER, " The Hepatic Microcirculation: Mechanistic Contributions and Therapeutic Targets in Liver Injury and Repair," *Physiol Rev*, vol. 89, 2009.
- [10] R. Sacco, V. Mismas, S. Marceglia, A. Romano, L. Giacomelli, M. Bertini, G. Federici, S. Metrangolo, G. Parisi, E. Tumino, G. Bresci, A. Corti, M. Tredici, M. Piccinno and L. Giorgi, "Transarterial radioembolization for hepatocellular carcinoma: An update and perspectives," *World Journal of Gastroenterology*, vol. 21, pp. 6518-6525, 2015.

- [11] A. Nicolini, S. Crespi and L. Martinetti, "Drug delivery embolization systems: a physician's perspective," *Expert Opinion on Drug Delivery*, 22 June 2011.
- [12] R. Loffroy, B. Guiu, J.-P. Cercueil and D. Krausé, "Endovascular Therapeutic Embolisation: An Overview of Occluding Agents and their Effects on Embolised Tissues," *Current Vascular Pharmacology*, vol. 7, 2009.
- [13] Cummins and Z. Herman, "Liquid, glass, gel: The phases of colloidal Laponite," *Journal of Non-Crystalline Solids*, 2007.
- [14] B. Ruzicka and E. Zaccarelli, "A fresh look at the Laponite phase diagram," *The Royal Society of Chemistry*, 2011.
- [15] BYK Additives & Instrumens, *LAPONITE – Performance Additives - Technical Information B-RI 21*.
- [16] N. Akarpovich, M. Vlasova, N. Sapronova, V. Sukharev and V. Ivanov, "Exfoliation Dynamics of Laponite Clay in Aqueous Suspensions Studied by NMR Relaxometry," *Oriental journal of chemistry*, vol. 23, no. 3, 2016.
- [17] B. Ruzicka, L. Zulian and G. Ruocco, "Routes to Gelation in a Clay Suspension," *PHYSICAL REVIEW LETTERS*, 2004.
- [18] Joshi, S. Jatav and M. Yogesh, "Chemical Stability of Laponite in Aqueous Media," *Elsevier B.V.*, 2014.
- [19] sigma-aldrich, *Product Information-Gelatin*.
- [20] A. K. Gaharwar, R. K. Avery, A. Assmann, A. Paul, G. H. McKinley, A. Khademhosseini and B. D. Olsen, "Shear-Thinning Nanocomposite Hydrogels for the Treatment of Hemorrhage," *ACSNANO*, vol. 8, no. 10, 2014.
- [21] O. Tacara, P. Sriamornsakb and C. R. Dassa, "Doxorubicin: an update on anticancer molecular action, toxicity and novel drug delivery systems," *Royal Pharmaceutical Society 2013 Journal of Pharmacy and Pharmacology*, vol. 65, 2012.

- [22] G. Wang, D. Maciel, Y. Wu, J. Rodrigues, X. Shi, Y. Yuan, C. Liu, H. Tomás and Y. Li, "Amphiphilic Polymer-Mediated Formation of Laponite®-Based Nanohybrids with Robust Stability and pH Sensitivity for Anticancer Drug Delivery," *ACS Applied Materials & Interfaces*, 2014.
- [23] A. C. Dunn, T. D. Zaveri, B. G. Keselowsky and W. G. Sawyer, "Macroscopic Friction Coefficient Measurements on Living Endothelial Cells," *Tribology letters*, vol. 27, p. 233–238, 2007.
- [24] S. Wang, Y. Wu, R. Guo, Y. Huang, S. Wen, M. Shen, J. Wang and X. Shi, "Laponite Nanodisks as an Efficient Platform for Doxorubicin Delivery to Cancer Cells," *Langmuir*, vol. 29, p. 5030–5036, 2013.